72275

Fragmental Polymict Breccia
St. 2,3640 g

INTRODUCTION

72275 is a fragmental breccia that may represent the matrix of Boulder 1, although it stood up in bold relief on the top of the boulder (see section on Boulder 1, St. 2, Fig. 2). It is predominantly light gray [N7], fairly friable, and encloses several protruding subrounded coherent knobs. Most such knobs are darker colored (medium gray [N51]. The sample was 17 cm long, and irregularly shaped with rounded corners. After collection it broke into several pieces (Fig. 1). The exposed surface had a thin patchy brown patina, with a few zap pits on some surfaces (N, E, B). Splashes of black glass covered some of the sample. An opposite face, tilted down toward the boulder, had a powdery covering that was layered and ripple-marked.

72275 is a porous aggregate of angular mineral, devitrified glass, and lithic fragments constituting a fragmental polymict breccia. The sample is not a regolith breccia. A few of the clasts are more than a centimeter across, including a conspicuous rimmed clast (Figs. 1, and 2) labeled Clast #1 or the Marble Cake clast. Other conspicuous clasts are the Apollo 17 KREEPy basalts (~3.93 Ga old) unique to this sample, many dark melt-matrix breccias, and varied feldspathic granulite and other feldspathic breccias. Numerous rock types,

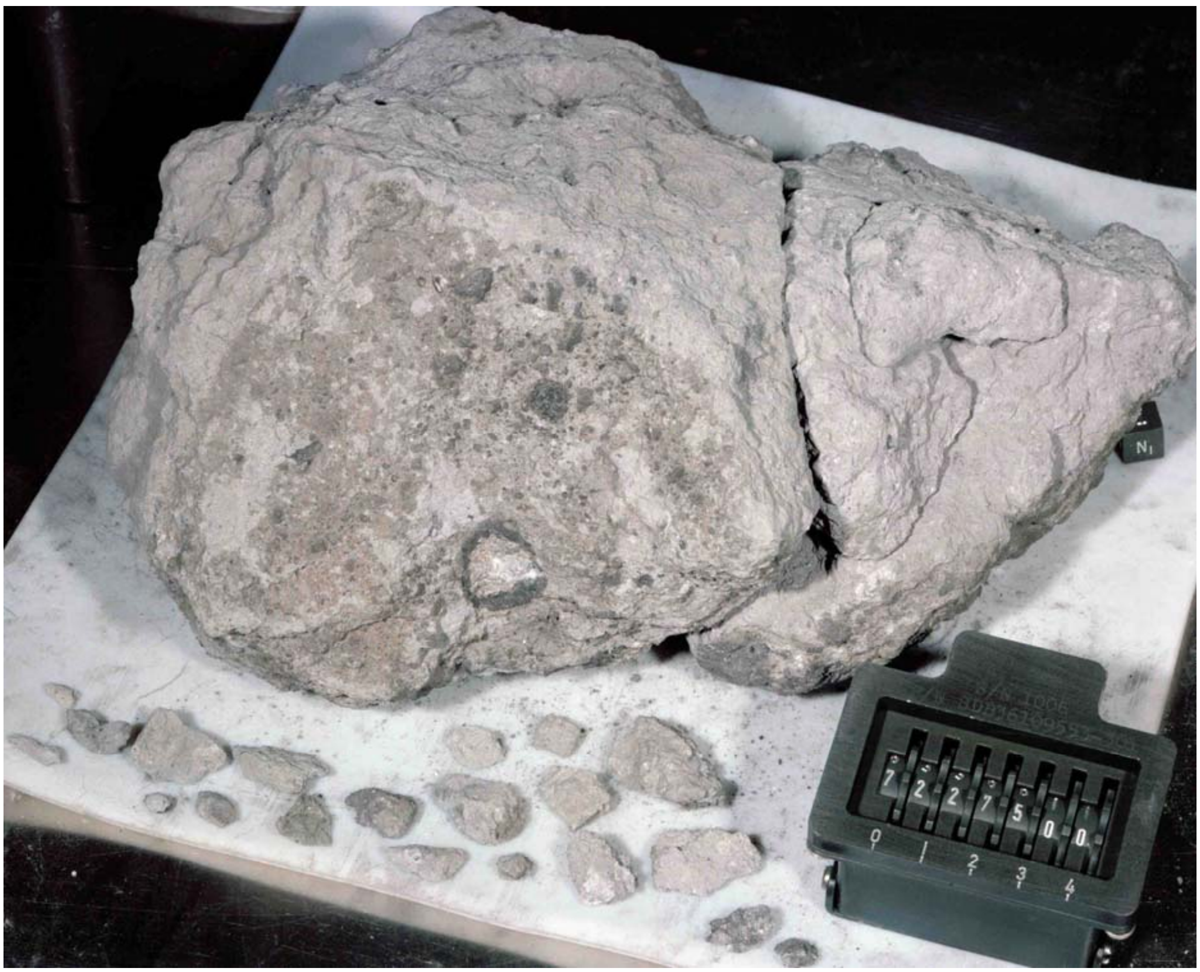

Figure 1: Reconstructed 72275, with documented pieces mainly on the right, and undocumented pieces in the foreground. The exposed north side shows thin brown patina. Clast #1 (Marble Cake clast) is prominent on the front face. Scale in centimeters. S-73-16077.

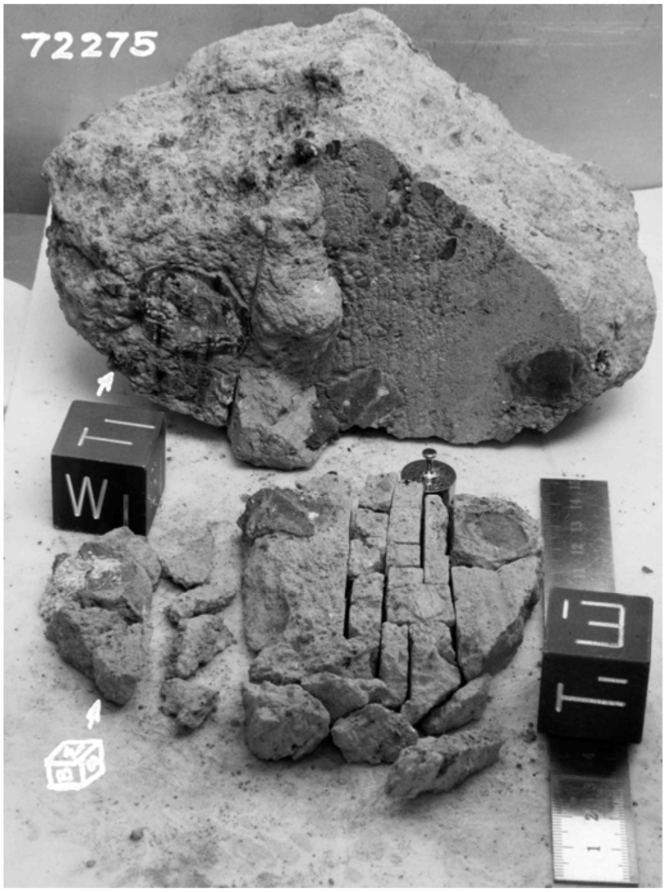

Figure 2: Initial slabbing and slab dissection of 72275, leaving irregular surface, and exposing the dark clasts #2 and #3. Gast #1 is to the left. Cubes are I inch. 5-73-34463.

such as other basalts, granites, and impact melts, are present as smaller fragments. Rare gas analyses suggest an exposure age of about 52 Ma, a little older than 72215 and 72255 and suggesting a two-stage exposure history for the boulder.

Most of the studies of 72275 were conducted by the Consortium Indomitable (leader J. A. Wood). A slab cut across the sample (Fig. 2) in 1973 made a comprehensive petrographic and chemical study possible. Detailed maps of the exterior surfaces and the slab based on the macroscopic observations, as well as descriptions of the sample allocations, were given in Marvin (in CI 1, 1974) (Fig. 3a, b). Two new slabs parallel to the rust were cut in 1984 (Figs. 3c, 4, 5) for new consortium studies (leader L. A. Taylor). They were described by Salpas et al. (1985).

PETROGRAPHY

72255 is conspicuously polymict (Figs. 1-5). LSPET (1973) described the sample as a layered light gray-breccia. Simonds *et al.* (1975) listed it as a fragmental breccia. The most detailed descriptions of the petrography of 72275 are given in Stoeser *et at.* (1974a, and in CI 1, Cl 2, 1974), Marvin (in CI 1, 1974), and Ryder *et al.* (1975b), who described 72275 as a light gray friable breccia. The Apollo 17 KREEPy basalts were described in particular by Ryder *et al.* (1977) and Salpas *et* al. (1987).

Mapping of the sample before and after slabbing (Marvin, in Cl 1, 1974) showed four main lithologic types (Fig. 3a, b)

1) the light gray matrix with minor darker gray zones, appearing as a friable aggregate of mineral and lithic clasts with a range of sizes up to about 0.5 mm. Plagioclase and a few percent brown and yellow mafic silicates were identifiable, with sparse grains of pink or amber spinel, and metallic iron.

2) anorthositic clasts of which the most conspicuous is clast #1 (Marble Cake clast), with a black rim. Smaller white clasts, with and without rims, occur throughout the specimen. Clast #1 is not pure white, but has 10 to 20% yellow mafic silicates, and appears to be a fluidized cataclastic breccia, interlayered with gray breccia and black rim material.

3) Dark gray aphanitic clasts, including clasts #2 and #3, which are hard, resistant dark gray materials (later identified as aphanitic impact melts). These clasts contain small angular fragments and thin white streaks indicating that they are polymict breccias. Small fragments are common in 72275.

4) Basaltic clasts and zones, which are the relics of the Apollo 17 KREEPy basalts. Most of the clasts

are rounded, and consist of white feldspar laths and yellow pyroxene. Most conspicuous are clasts #4 and #5 on the slab pieces. The clasts are embedded in zones of fine-grained basaltic debris, but these zones are difficult to delineate macroscopically. (Other basaltic clasts were later found and mapped on the newer slab cuts by Saipas et al., 1985, 1987).

Three distinct lithologic units in the 1984 surfaces were recognized by Willis (1985). A darker and coarser unit separated two lighter, more fine-grained units. Each is distinct with respect to clast sizes, abundance, and types. One of the lighter units consists mainly of basalts sitting in crushed basalts, whereas the other changes from breccia clasts (mainly dark melt breccias) to basalts towards the interior of the rock. The dark coarse zone consists mostly of dark melt breccia clasts. In all the units the average clast dimension decreases from the first face exposed to the last.

Stoeser et al. (1974a, and in Cl 1, 1974) and Ryder et al. (1975b) considered that the sample had two major lithologic types, that of the gray polymict breccia, and that of the KREEPy basalt (which they referred to as "pigeonite basalt") breccia; the latter forms about 30% of the exposed surfaces. The light-gray friable breccia is composed of porous, poorly-sintered matrix, with angular mineral and lithic clasts (Fig. 6a, b). A clast population survey was tabulated by Stoeser et al., (1974a) (Table 1); however, this table omits the dark matrix breccias (the aphanitic melts) that are the dominant clast type. The dark aphanitic melts, which resemble samples 72215 and 72255 in petrography and chemistry, are themselves polymict, containing all the other clast types except for the KREEPy basalts. Materials similar to the Civet Cat norite and granites appear to be dominantly, if not absolutely, confined to the dark aphanitic melts. Neither glass spherules or

Table 1: Population survey of clast types in 72275 light gray matrix, excepting the dark impact melt breccias. % by number, not area. (Stoeser et al., 1974a).

Clast type	72275
Granulitic ANT breccias	48.3%
Granulitic polygonal anorthosite	3.5
Crushed anorthosite	5.1
Devitrified glass	7.9
Glass shards	0.4
Ultramafic particles	1.6
Basaltic troctolite	2.0
Pigeonite basalt	5.1
Other basaltic particles	2.0
Granitic clasts	1.6
"Civet Cat" type norite	0.4
Monomineralic plagioclase	15.0
Monomineralic mafic silicates	5.5
Monomineralic spinel & opaques	1.2
Number of clasts surveyed	254

ropy glass clasts, nor their devitrified equivalents that are characteristic of regolith breccias, occur in the light-gray friable matrix. The range of mineral fragments (Figs. 7-9) is similar to the range in the dark aphanitic melts (Figs. 9, and 10), with plagioclase, low-Ca pyroxenes, and olivine predominant. ilmenite, troilite, Fe-metal, pink spinel, chromite, and trace amounts of K-feldspar, silica, zircon, and armalcolite, are present. The differences in lithic clast populations preclude the possibility that the light-gray friable matrix is a crushed version of the dark aphanitic melts. The lack of equilibration rims and lack of extensive sintering suggest that the light-gray matrix was not subjected to high temperatures for any great length of time.

A17 KREEPy Basalts:

The KREEPy basalts, originally referred to as Pigeonite basalts (Stoeser et al. in CI 1, 1974, and 1974a,b) occur as fragments and breccia zones in the light gray matrix (Fig. 3a,b). They have not been found in the dark impact melt breccias, nor in any other samples. The brecciated zones consist almost entirely of crushed basalts, and are clots or bands up to 2 cm thick. (Marvin, in C' 1, 1974; Stoeser et al., in Cl 1, 1974). The clasts are rounded, with prominent white feldspar and yellow mafic silicates. Few of the relict basalt fragments are more than a few millimeters across; rare examples reach one centimeter.

Most of the KREEPy basalts clasts have a mesostasis-rich subophitic to intersertal texture (Fig. 6e) (Stoeser et al., CI 1, 1974; Cl 2, 1974, l 974a,b; Ryder et al., 1975b, 1977; Irving, 1975; Salpas et al., 1985, 1986a, 1987). Most have a medium grain size (silicates 500-1000 microns), but there is a range down to fine-grained equigranular and glassy vitrophyric varieties, which are less common. The textures are homogeneous, and the fragments contain no xenoliths or other features suggestive of an impact origin for the melt phase. The chemical evidence (below) also suggests that these basalts are volcanic. The range in grain sizes and textures suggests that a sampling of both flow interiors and exteriors was obtained. The dominant subophitic basalts consist of approximately equal amounts of plagioclase and clinopyroxene (mainly pigeonite), with 10% to 30% of a complex fine-grained and opaque mesostasis (Fig. 6e). A

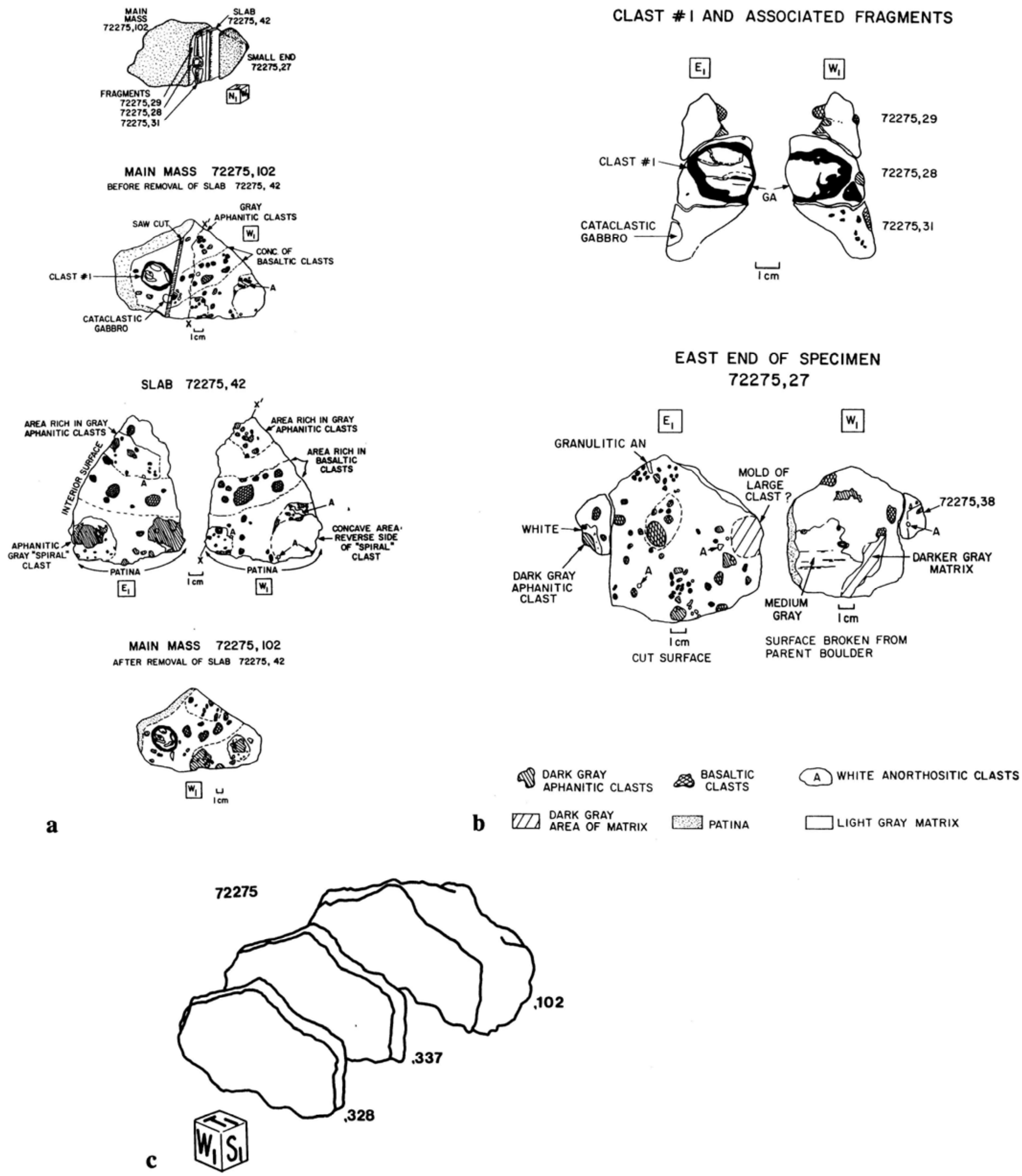

Figure 3: Slabbing and mapping of 72275. a) Sawn surface of the main mass (, 102), and the slab (, 42). b) Surface of clast #1 and the east end piece (, 27). c) 1984 reslabbing of main mass, 102. Cube is 1 inch.

Figure 4: Exposed west face of first 1984 slab (,328) after removing irregular surface left in 1973 slabbing. Most of the surface visible is that exposed in Fig. 2; another large clast has been exposed. Cube is I inch; rule scale is centimeters. S-84-45540.

Figure 5: Exposed east face of second 1984 slab (,337) and its subdivisions. There is an obvious lack of large clasts compared with the earlier exposed faces. Cube is I inch; rule scale is centimeters. S-84-46145.

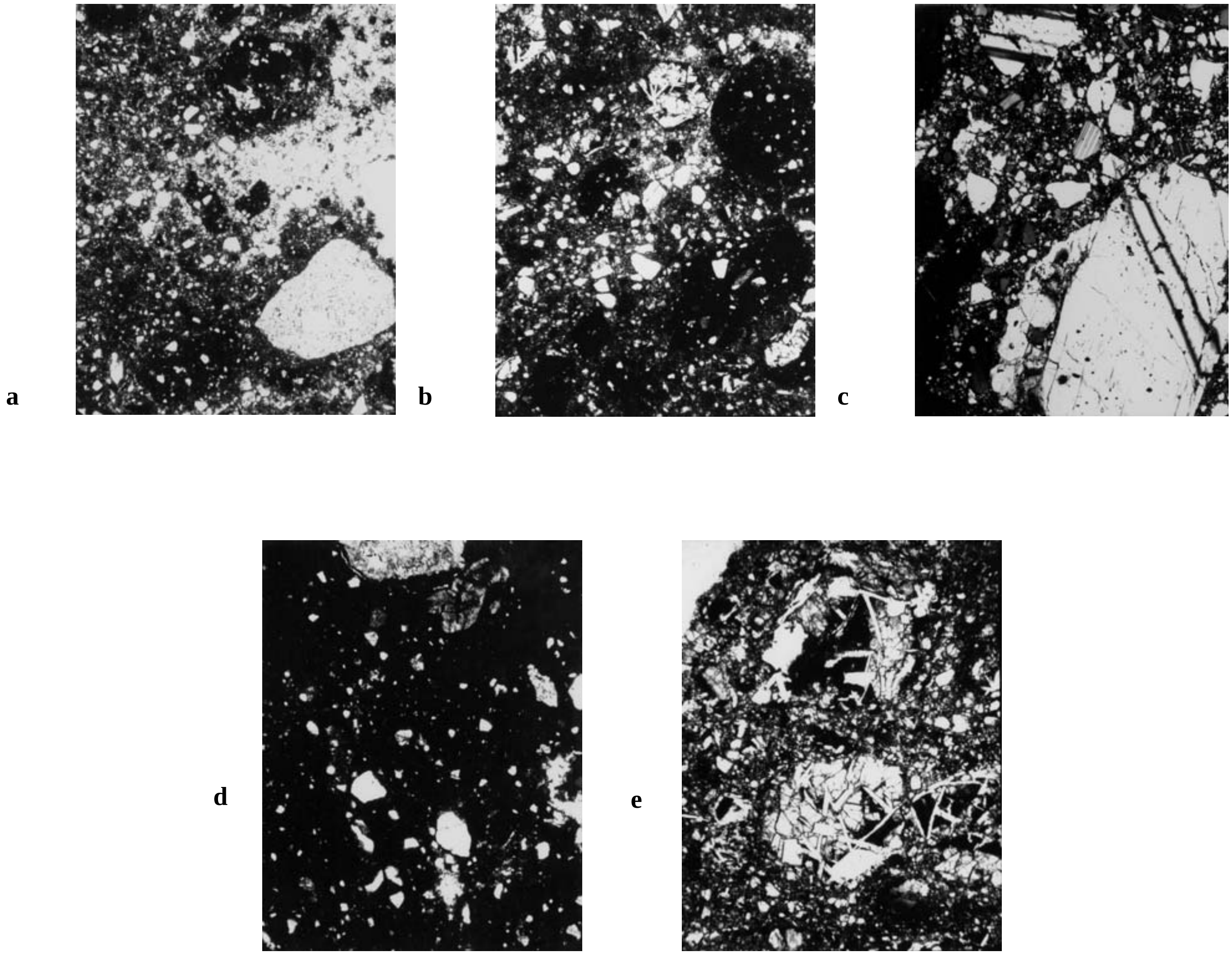

Figure 6: Photomicrographs of 72275. All plane transmitted light except c), crossed polarizers. All about 2mm field of view.

a) 72275,13: general friable matrix of undocumented chip, showing feldspathic granulite clasts and schlieren (right), clasts or blobs of dark melt matrix breccias, and numerous mineral clasts.
b) 72275,134: general matrix of 1973 slab near clast #5, showing rounded dark melt breccia pieces, mineral clasts, and small fragments of KREEPy basalts
c) 72275,138: anorthositic breccia from the core of clast #1, the Marble Cake clast.
d) 72275,145. matrix of clast #2, a dark melt breccia.
e) 72275, 147: clast #5, a monomict breccia or cataclasite of KREEPy basalt.

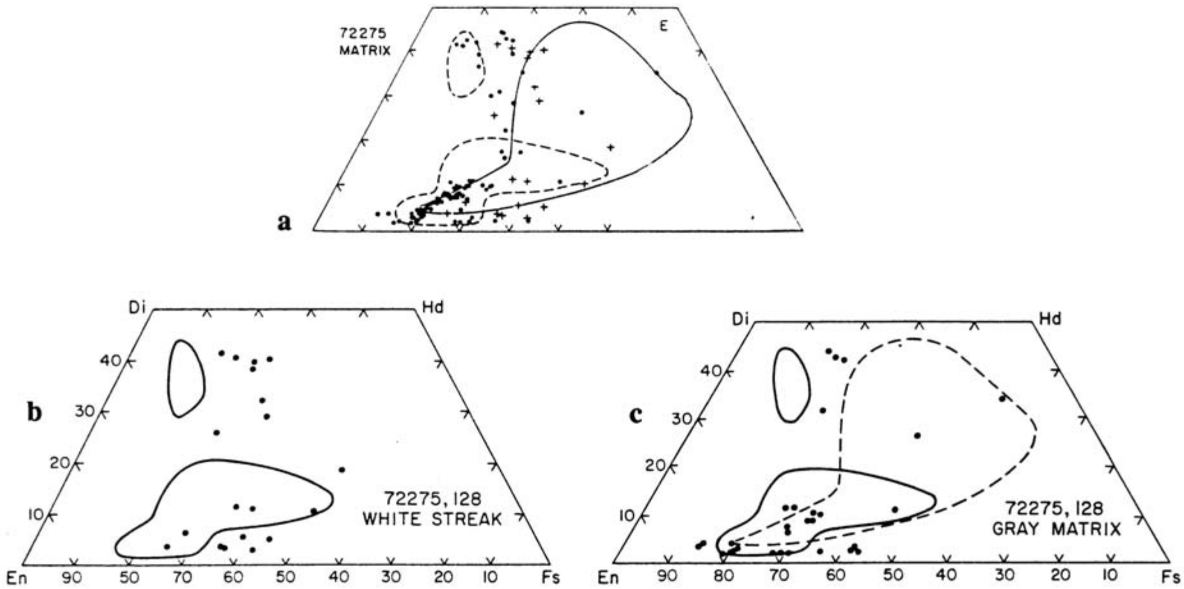

Figure 7. Compositions of pyroxenes in 72275 light gray friable matrix samples. The large outlined area is the range of compositions of pyroxenes in the KREEPy basalts; the smaller outlined areas are the ranges for anorthositic breccias. a) b) are general matrix, c) is a white streak in the matrix in,128 a) from Stoeser et al. (1974a). b) c) from Stoeser et al. in C11, 1974.

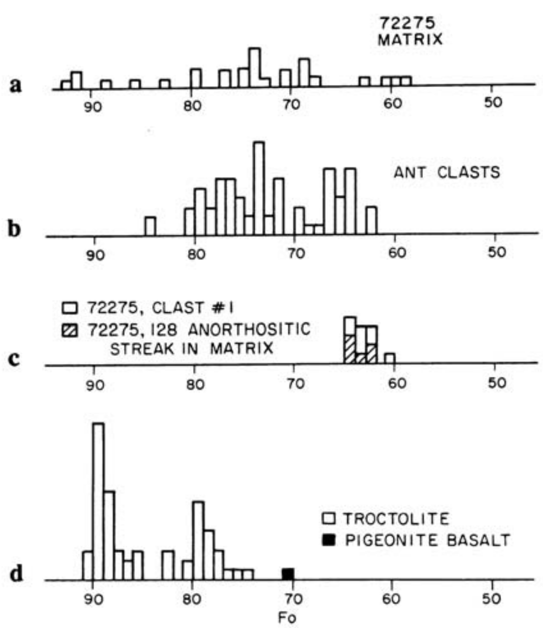

Figure 8: Histograms of olivine compositions in 72275 matrix and clasts. a) monomineralic olivines in general light gray matrix. b) olivines from feldspathic granulite clasts. c) olivines in clast #1 and the white streak in ,128. d) olivines in the troctolitic basalts (impact melts?) and the KREEPy basalts (= pigeonite basalts). Stoeser et al. (1974a).

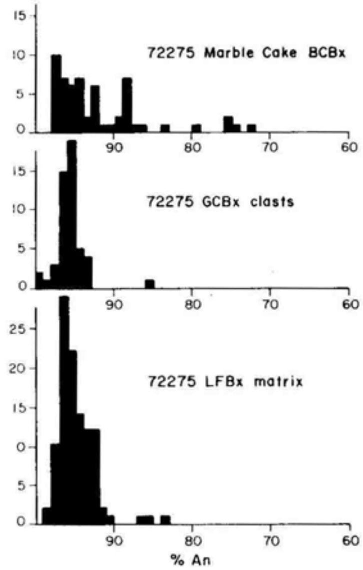

Figure 9: Compositions of olivines in 722751ithologies. Marble Cake is clast #1; GCBx are the dark impact melt breccias; LFBx is the general light gray matrix. Ryder et al. (19756).

silica mineral (cristobalite?), minor chromite, Fe-metal, and very rare olivine are present outside of the mesostasis. The mesostasis consists of ilmenite, Fe-metal, cristobalite (?), plagioclase, ferroaugite, phosphate, troilite, potash feldspar, zircon, and a Si-rich glass. Both Fe-metal and troilite occur as veins.

The compositions of silicate mineral phases are shown in Figs. 11, 12, and 13, and analyses of metal grains in Fig. 14. Representative microprobe analyses of phases are tabulated in Stoeser *et al.* (in Cl 1, CI 2, 1974; 1974b; Ryder *et al.*, 1977). Phases in the relict basalt fragments and the brecciated zones show similar ranges (e.g. Figs. 11, and 12).

Plagioclases, which form an interlocking network of laths, is zoned normally; the trend towards extreme Or-enrichment in plagioclase appears to be unique among lunar samples. Some of the plagioclase borders contain glassy or microcrystalline silicic globules less than l0 microns in diameter, possibly trapped magma (Ryder *et* al., 1977. Clinopyroxene, which encloses plagioclases, is elongate to tabular. Many are twinned; none are sector zoned. The first pyroxene to crystallize was Mg-pigeonite; orthopyroxene such as is common in A 15 KREEP basalts is absent. Zoning to more Fe-, Ca-rich pyroxenes is commonly erratic.

The silica polymorph is a late-stage phase, and composes as much as 5% of some clasts. It has the mosaic fracture pattern characteristic of cristobalite. Some grains are laths (poorly-developed) and up to 500 microns long. Chromite is a euhedral to subhedral early-crystallizing phase, most less than 50 microns, that is aluminous and zoned to titanian chromite rims. Olivine is rare, small (less than 300 microns), and a compositional range from Fo69-64. It appears to have survived by enclosure in other silicates. The mesostasis forms interstitial triangular patches several hundred microns across. There is no evidence of immiscibility, although it is heterogeneous, appearing to be more Fe-rich adjacent to pyroxene and more silicic adjacent to plagioclases (Stoeser et al., in Cl 1, 1974). The mesostasis rims are not all sharply defined. The bulk composition of the mesostasis is Fe-, Si-, and P-rich, and poor in K compared with many other lunar mesostasis compositions. Fe-metal and (less common) troilite occur in the mesostasis, as veins, and as blebs in early-crystallizing phases. Their low Ni contents are consistent with lack of meteoritic contamination and thus, a volcanic origin for the basalts.

Dark Impact Melt Breccias: Materials originally labeled "dark matrix breccias" (Stoeser et at. , in Cl 1, 1974) and later gray to black competent breccias (e.g. in Ryder et al., 1975b) are a distinctive feature of 72275. They are the dominant clast material, and occur as discrete clasts and as rinds to, or intermixed with, feldspathic clasts such as feldspathic granulites. They are similar to the dark matrix materials that form the other Boulder 1 samples 72215 and 72255, and were similarly eventually recognized as aphanitic impact melts (e.g. Ryder and Wood, 1977; Spudis and Ryder, 1981) and not the metamorphosed breccias originally suggested (e.g. Stoeser et al., 1974a, Ryder et a1., 1975b). They are also similar to the Station 3 samples 73215, 73235, and 73255 (e.g. James et al., 1978). The dark breccias were described by Stoeser et al., (1974a,b, and in CI 1, Cl 2, 1974), Ryder et al. (1977b), and Spudis and Ryder (1981).
Most of the dark melt breccias are less than 1 mm, but some are much larger, including Clasts #2 and #3 exposed on the sawn faces (Fig. 2-4). Clast #3 was not allocated, but clast #2 was allocated for petrographic and chemical studies. The Marble Cake clast (clast #1) is a complex rimmed clast (see below). Clasts #1 and #2, and many of the smaller dark breccias, have a "globby" nature, with rounded and irregular outlines (Figs. 2, 4, and 6a, b). In thin sections they are very dark and dense, with a very fine-grained groundmass enclosing a variety of clasts, usually small (Figs. 6a, b, d). The lithic clast population consists of feldspathic granulites, other feldspathic breccias, some basalts and coarser impact melts, and sparse granites. Monomineralic clasts are mainly plagioclase, but olivines and pyroxenes are also common. Some dark clasts have vesicles. The melt matrices are fine-grained, mainly plagioclase and probably pyroxene commonly less than 5 microns, and the melt fraction is probably about 50-70% of the volume. Compositions of monomineralic silicate phases, mainly clasts, are shown in Fig. 9b (plagioclases) and Fig. 10 (olivines and pyroxenes). The range in compositions of mafic minerals is greater than that of anorthositic breccias (e.g. granulites), and indicates that a wide variety of lithologies contributed to the dark melt breccias. However, no fragments of the A 17 KREEPy basalts have been found in these melt breccias. Defocused beam

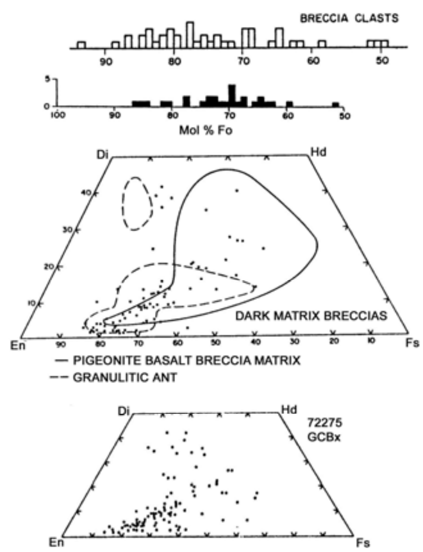

Figure 10: Figure 10: Compositions of olivines (a, b) and pyroxenes (c, d) in dark impact melt breccias (GCBx) in 72275. a) Stoeser et al. (1974x), b),d) Ryder et al. (1975b), c) Stoeser et al., CI 1.

analyses (Table 2) show that the dark matrix breccias have low-K Fra Mauro basalt compositions similar to those in 72215 and 72255 (see also chemistry section), suggesting a common source, although there is some variation.

Clast #1 (Marble Cake):
The distinctive 3 cm clast visible on the north face (Fig. 1) and after slabbing (Figs. 2-4) was described by Stoeser et al. (1974x, and CI 1 and CI 2, 1974), Marvin et al. (1974), and Ryder et al. (1975b). It consists of a light-colored core (white, with about 10 to 20% yellow minerals) with a dense envelope of dark brachia material that also is crudely interlayered with the core. The rim and the core have been fluidized simultaneously. Part of the clast was thin sectioned and mapped (Fig. 15). Compositions of mafic mineral phases are shown in Fig. 16. Defocused beam analyses of some clasts are given in Table 3. The dark breccia consists of an aphanitic impact melt, similar to other dark breccias in 72275 except that it is darker, more vesicular, and higher in K and P than most (Table 2, col. 9) (Stoeser et al., in CI 2, 1974). The core material is a complex mix, dominated by a coarse-grained feldspathic lithology that has been crushed (Fig. 6c). Some of its fragments are granulitic, and more than one feldspathic rock type may be present. The parent rock was plagioclase-rich (more than 80%), and contained olivine (Fo_{60-68}), bronzite, and augite: a cataclastic troctolitic ferroan anorthosite. Ilmenite microgabbros are small igneous (or possibly metamorphic) fragments that are fine-grained and not reported from other lunar samples; they consist of 43-57% plagioclase (An_{65-80} Or_{5-15}), 25-46% pyroxene (Mg' about 50; see Fig. 16), and 9-18% ilmenite. They also contain minor amounts of cristobalite, troilite, and metallic iron. They are more similar to sodic ferrogabbro fragments at Apollo 16 (Roedder and Weiblen, 1974) than other samples, but are actually unique. Some exsolved pyroxene fragments that are 200 microns across (hence bigger than those in the ilmenite microgabbros) have a composition similar to those in the ilmenite microgabbros; their source could be a coarser-grained equivalent. Other clast types include an orange glass (spinel troctolite composition), some fine-grained "basalts" with quenched appearance that give the impression of being impact melts, and microgranites. The latter are fairly common.

Feldspathic Breccias:
72275 contains a variety of feldspathic lithic materials ranging from cataclastic ferroan anorthosite-like materials to feldspathic granulites; some of them reach several centimeters long. Apart from the dark melt breccias (in which they are a clast-type), they are the most abundant clasts in 72275; they also occur as discrete fragments in the light gray friable breccia. The feldspathic clasts were described by Stoeser et al. (1974a, and in C11, CI 2, 1974), and by Ryder et al. (1975b) under the now-obsolete acronym ANT (anorthosite, norite, troctolite). Some are several centimeters in size, and are petrographically similar to those found in other Boulder 1 samples and elsewhere at the Apollo 17 site. Recrystallized varieties (feldspathic granulites, both poikilitic and granulitic in texture) are most common. The compositions range from noritic to troctolitic anorthosites. They have a range of mineral compositions (e.g. Fig. 17), though most individual clasts are fairly well-equilibrated. The ranges are not unlike those reported for other feldspathic highlands breccias; they do not include mafic minerals with Mg' much higher than 0.83, and the plagioclases are dominantly very calcic.

The samples described by Stoeser et al. (1974a, and in CI 1, CI 2, 1974) and Ryder et al. (1975b)

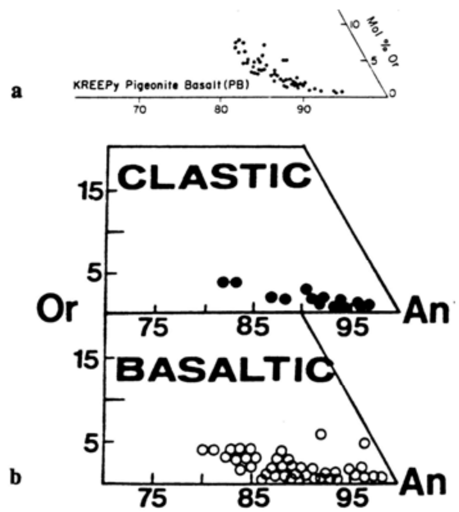

Figure 11: Compositions of plagioclases in A 17 KREEPy basalts. a) Ryder et al. (1975b) b) Salpas et al. (1985, 1987). Clastic refers to plagioclases in comminuted zones.

were classified as unrecrystallized, granulitic, and poikiloblastic "ANT" breccias. Poikilitic fragments are rare to absent. The unrecrystallized fragments have porous fragmental matrices, and appear to be crushed anorthositic igneous rocks. The dominant part of the core of the Marble Cake clast is one such fragment. The granulitic fragments are characterized by triple point textures typical of recrystallization. Their compositions and textures are varied. Poikiloblastic fragments are distinguished by their small poikilitic pyroxenes enclosing smaller plagioclases, set in a mosaic of much coarser plagioclases; all are fine grained, with even the larger plagioclases rarely more than 200 microns. Salpas el al. (1986b, 1987a) described an anorthositic clast from the 1984 slabbing that they referred to as the first Apollo 17 ferroan anorthosite; however, there are other candidates for that honor (including the core of the Marble Cake clast, which is certainly closely related). The small fragment (less than 5 mm) is monomict, consisting of about 95% anorthite $_{(An95.1-97.1)}$ and 5% pyroxene (augite and pigeonite; Fig. 18). The pyroxene occurs as small (less than 100 micron) grains interstitial to larger plagioclases. Salpas et al. (1986b, 1987a) also described six feldspathic granulite clasts from the 1984 slabbing. Their characters are summarized in Table 4. In general they are composed of rounded to angular fragments of plagioclase and olivine in granoblastic or poikiloblastic matrices of plagioclase and pyroxene. The amount of olivine is rather small (e5%). The textures of the granulites suggest that most are brecciated assemblages which were subsequently recrystallized.

72275 also contains small amounts of other lithic clast types, ranging from olivine-normative mare basalt-like fragments, ultramafic particles, troctolitic basalts (probably impact melts), and granitic fragments (Table 1).

CHEMISTRY

A large number of chemical analyses have been made on 72275 matrix and its clastic components, ranging from fairly comprehensive analyses to analyses for one or two elements as part of geochronological studies. The chemical data are given in Tables 5a,b,c (light gray matrix and dark melt breccias), Tables 6a, b (KREEPy basalts), Table 7 (Clast # 1, Marble Cake, lithologies), and Table 8 (feldspathic breccia clasts). The data given by Jovanovic and Reed (several papers) includes some combined leach and residue data.

Light gray friable matrix and dark melt breccias:
The several analyses of bulk friable matrix show some variability at the scale of the rather small samples generally analyzed (less than 50 mg) (Tables 5a, b; Fig. 19). The chemistry differs from that of the dark melt breccias and from other boulder matrices at the Apollo 17 site in being less aluminous and more iron-rich. The chemistry is consistent with a mix of dark melt breccias, feldspathic breccias, and KREEPy basalts. The latter component is seen in the very high Ge content of the matrix (Morgan *et al.*, 1974, 1975), as high Ge is a distinctive character of the KREEPy basalts. The matrix analyses reported by Salpas *et al.* (1987b) are identical in all respects with the KREEPy basalts themselves and these samples must have very low contents of feldspathic granulites or melt breccias. Their abundances of incompatible elements (Fig. 19b) is higher than most other matrix samples and similar to those in the KREEPy basalts (Fig. 20).
Of the dark melt breccias, only clast #2 (Table 5c) and the Marble Cake rind (below) were analyzed, apart from the defocused beam microprobe analyses (the defocused beam analysis of clast #2 agrees tolerably well with the atomic absorption analysis except for its higher normative feldspar). The

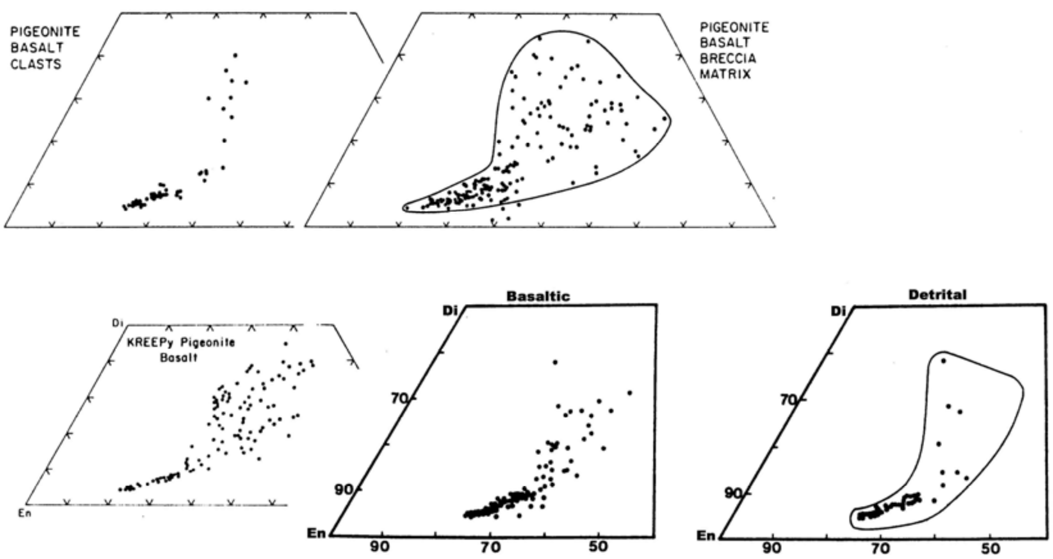

Figure 12: Compositions of pyroxenes in A 17 KREEPy basalts and breccias, plotted on quadrilaterals. a) Stoeser et al. (1974). b) Ryder et W. (1977). c) Salpas et al. (1987)

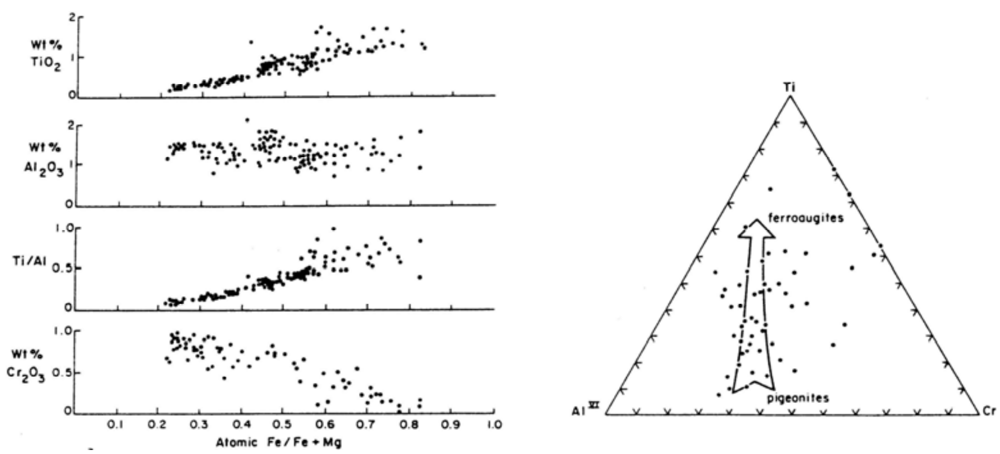

Figure 13: Abundances and ratios of minor elements in pyroxenes in A 17 KREEPy basalts. Arrow indicates direction of crystallization. Ryder et al. (1977).

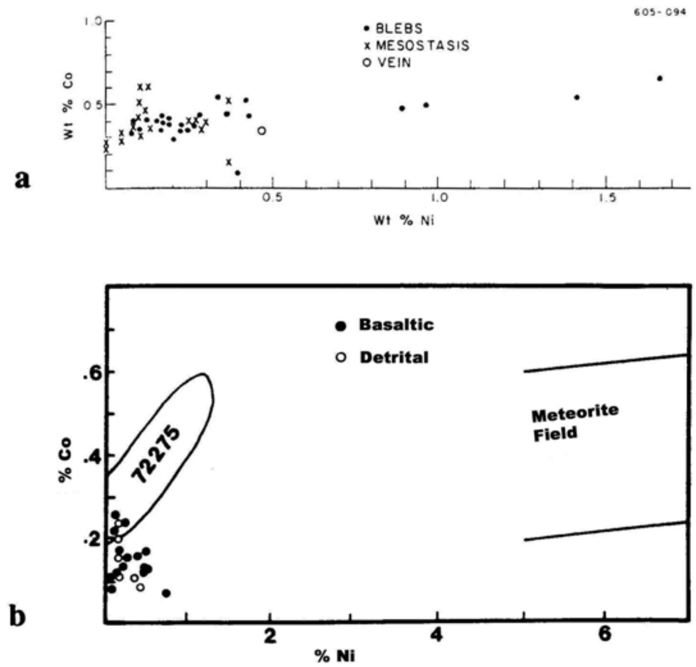

Figure 14: Compositions of metals in A 17 KREEPy basalts. a) Ryder et at. (1977), b) Salpas et al. (1987). In b) field labeled "72275" is taken from a) and the difference is stated by Salpas et al. (1987) to be an analytical problem in the Ryder et al. (1977) study.

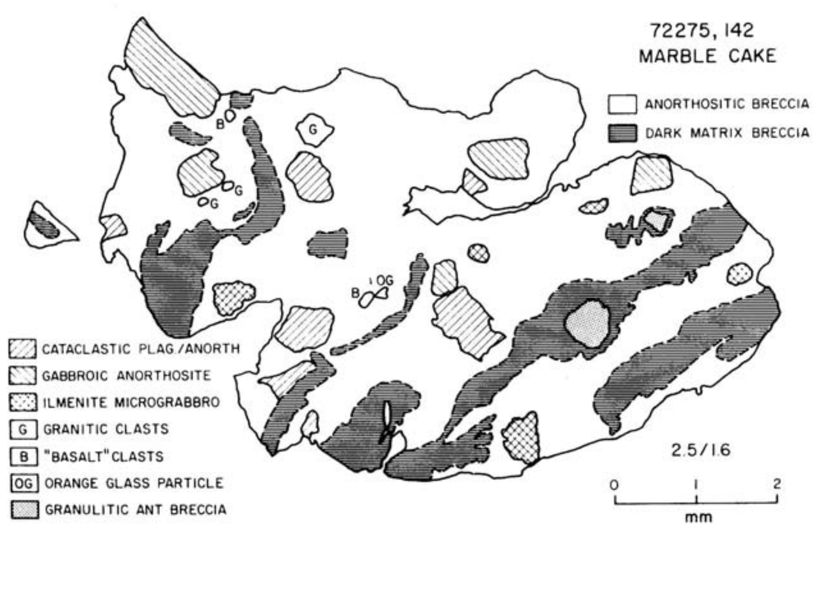

Figure 15: Sketch map of the interior of clast #1 (the Marble Cake clast). The white areas consist of a mixture of finely-crushed gabbroic anorthosite and ilmenite microgabbro. Uncrushed remnants large enough to map are indicated by clast type. Stoeser et al. (in C12, 1974) and Marvin et al. (1974).

Table 2: Defocused beam electron microprobe analyses of dark aphanitic melt breccias in 72275.
Key: 5) 72275,128, average of 10 analyses of 2 clasts. 6) 72275,134, average of 21 analyses of clast. 7) 72275,12, average of 5 analyses of rind around anorthositic clast. 8) Clast #2, average of 15 analyses. 9) Dark melt material of clast #1 (the Marble Cake clast). (Stoeser et al., in CI 1, 1974).

	5	6	7	8	9
	72275, 128 DMB matrix	72275, 134 DMB matrix	72275, 12 vesicular rim	72275, 146 clast #2 matrix	72275, 140 DMB
SiO_2	49.7	47.7	43.9	47.0	46.6
TiO_2	1.1	1.1	0.9	1.0	1.3
Cr_2O_3	0.2	0.2	0.2	0.2	0.2
Al_2O_3	18.8	20.3	22.9	22.8	19.6
FeO	10.0	10.6	8.7	8.9	11.0
MnO	0.1	0.2	0.1	0.1	0.2
MgO	9.0	10.0	12.1	8.7	8.2
CaO	11.4	11.5	11.6	12.9	11.4
Na_2O	0.5	0.5	0.7	0.6	0.6
K_2O	0.3	0.2	0.3	0.2	0.5
P_2O_5	0.5	0.4	0.3	0.5	0.8
Total	101.6	102.7	101.7	102.9	100.4
Fo	0.0	3.4	16.5	4.5	1.6
Fa	0.0	2.7	8.8	3.3	1.5
En	22.0	19.5	6.1	14.8	18.2
Fs	16.3	13.9	3.0	9.9	15.5
Wo	2.1	0.7	0.0	0.8	1.1
Or	2.0	1.3	1.6	1.3	2.9
Ab	3.9	4.2	5.4	4.9	5.5
An	47.5	51.1	55.1	57.4	48.7
Ilm	2.1	2.0	1.6	1.8	2.5
Chr	0.3	0.3	0.3	0.3	0.3
Qtz	2.7	0.0	0.0	0.0	0.0
Cor	0.0	0.0	1.0	0.0	0.0
Ap	1.1	1.0	0.6	1.0	1.8

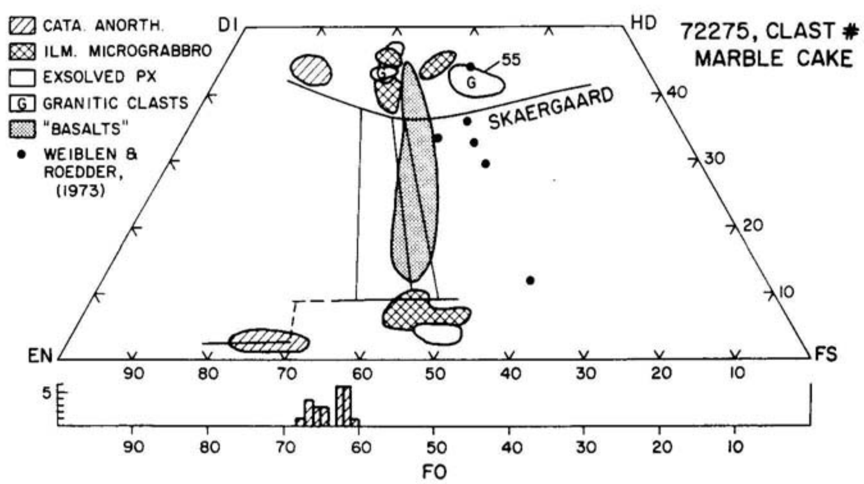

Figure 16: Compositions of pyroxenes and olivines in phases of the interior of clast #1 (the Marble Cake clast) and sodic ferrogabbros for comparison.

Table 3: Defocused beam electron microprobe analyses of four types of clast in the light-colored interior of clast #1 (the Marble Cake clast).
(Stoeser et al., in Cl 2,1974).

		1.	2.	3.	4.	5.	6.
		790C10 anorth. gabbro	790C18 gabbroic anorth.	790C1 ilmenite microgab.	790C2 ilmenite microgab.	790C5 "basalt"	790C6 orange glass
WT. % OXIDES							
SiO_2		43.38	41.16	45.89	48.48	47.10	43.20
TiO_2		0.08	0.06	4.38	6.59	2.89	0.26
Al_2O_3		20.87	29.96	14.70	14.54	10.09	13.96
Cr_2O_3		0.06	0.03	0.05	0.05	0.11	0.05
FeO		7.85	4.16	11.70	10.01	15.19	8.49
MnO		0.13	0.04	0.17	0.14	0.19	0.05
MgO		8.79	3.56	5.67	3.38	7.32	22.87
CaO		12.70	16.01	12.16	9.42	13.08	8.96
Na_2O		0.28	0.26	0.91	0.85	0.37	0.66
K_2O		0.05	0.05	0.92	0.90	0.25	0.23
BaO		0.04	0.04	0.11	0.11	0.09	0.04
P_2O_5		0.02	0.03	0.46	0.42	0.35	n.d.
TOTAL		94.29	95.43	97.27	95.05	98.02	98.81
CIPW NORM							
FO		6.1	5.3	---	---	---	38.5
FA		4.4	4.9	---	---	---	11.3
EN		14.5	1.8	14.5	8.9	18.7	2.7
FS		9.6	1.5	14.6	7.7	20.6	0.7
WO		3.3	---	10.3	4.8	16.1	4.2
OR		0.3	0.3	5.6	5.6	1.5	1.4
AB		2.5	2.3	7.9	7.6	3.2	5.6
AN		58.9	83.1	34.3	35.0	25.8	34.9
ILM		0.2	0.1	8.6	13.2	5.6	0.5
CHR		0.1	---	0.1	0.1	0.2	0.1
QTZ		---	---	2.7	15.8	5.3	---
COR		---	0.4	---	---	---	---
AP		0.1	0.1	1.1	1.0	0.8	---
COMP. NORM MIN.							
OL:	FO	66.5	60.7	---	---	---	83.2
PX:	EN	58.9	60.7	42.0	47.0	39.0	39.2
	FS	29.7	39.3	32.2	31.1	32.1	7.9
	WO	11.4	---	25.8	21.8	28.9	52.9
PLAG:	OR	0.5	0.3	11.5	11.5	5.0	3.3
	AB	4.3	2.9	17.4	16.5	11.0	14.1
	AN	95.3	96.8	71.0	72.0	84.0	82.6
atomic Mg/(Mg+Fe)		0.666	0.604	0.463	0.375	0.462	0.827
MgO/(MgO+FeO)		0.528	0.461	0.326	0.252	0.325	0.729
No. of analyses		26	16	12	4	3	1

clast # 2 analysis is similar to those for 72255 and 72215 dark melt breccias except for slightly higher abundances of incompatible elements (the Marble Cake rind has even higher abundances of incompatible elements). Blanchard et al. (1975) described clast #2 as intermediate in chemistry between the rind material and more typical dark melt breccias such as those in 72255.

The 72275 brecciated materials have obvious meteoritic contamination (Morgan et at, 1974, 1975). Morgan et at (1975) grouped the meteoritic materials in 72275 and 72255 as distinct from those in the other Boulder 1 samples: Group 311, and 3L for the 72215 and 72235 samples. Ali are distinct from most other Apollo 17 samples (Group 2). The distinctions are not a result of the high Ge in the KREEPy basalts. Jovanovic and Reed (e.g. 1975c) interpreted their data on some volatile elements as constraining the thermal history of Boulder 1: since consolidation it probably has not been subjected to temperatures greater than 450 degrees C, and vapor clouds from external sources permeated the source regions for the boulder materials.

A 17 KREEPy BASALTS: Analyses of the KREEPy basalts sampled from the 1973 sawing (clast 5 and probably clast 4) are given in Table 6a, and numerous analyses of small clasts (mainly basaltic breccia) sampled from the 1984 sawing in Table 6b. Most of the latter are partial analyses. The rare earths are shown in Fig. 20. The KREEPy basalt is quartz-normative, with an evolved Mg' similar to some mare basalts, but with elevated rare earths compared with mare basalts. The sample lacks meteoritic contamination (Morgan et at, 1974, 1975). The rare earth elements are KREEP-like, but the heavy rare earths have a slightly steeper slope than other KREEP basalts. These basalts cannot be related to other known KREEP basalts by fractional crystallization or partial melting of common sources. They are quite distinct from the only other volcanic KREEP samples known, the Apollo 15 KREEP basalts (Ryder et at, 1977; Irving, 1975). Ryder et at (1977) discussed the chemistry as being intermediate between mare and KREEP basalts. Salpas et at (1987b) found that the breccias and the actual basalt clasts were indistinguishable in composition. They interpreted their analyses to represent fragments of a single flow or of a series of related flows, with a fairly consistent trend on an 01-Si-An diagram for the 9 samples that they analyzed more completely (Fig. 21). However, this diagram may be misleading: Some of the variation that they found undoubtedly results from unrepresentative sampling, and the Si02 abundances are obtained by difference, not analysis. The trend on the diagram is not that of pyroxene or pyroxene + plagioclase (as the petrography would indicate), but of olivine control; it may be an artifact.

The very high Ge content of the KREEPy basalt is distinctive, and is accompanied by lesser enrichments in Sb and Se (Morgan et al., 1974, 1975).

Clast #1 (Marble Cake clast): Analyses of both white and dark portions of the Marble Cake clast are given in Table 7, with the rare earth elements shown in Fig. 22. Both phases are polymict, although the white material is dominantly a cataclastic troctolitic anorthosite/feldspathic granulite, and the dark material is dominantly an aphanitic melt breccia. The analysis of the white material probably includes some dark melt component (Blanchard et al., 1975) and presumably ilmenite microgabbros and other lithologies. The rare earth element abundances are higher than expected for anorthositic or granulitic rocks. The dark rim material contains much higher incompatible element abundances than most other dark melts in the boulder, this includes Rb, U, and Th as well as the rare earths. These abundances are higher than their counterparts in the KREEPy basalts and are more similar to the levels in A14 or A15 KREEP. The rim and the core are absolutely distinct in composition; the rim is not melted core, but appears to be plastered on in flight, as suggested by Stoeser et al. (1974a). The rim material contains meteoritic contamination, but no analysis for meteoritic siderophiles was made for the core. The rim siderophiles have ratios corresponding with group 3 siderophiles that characterize other boulder matrix samples.

Feldspathic breccias:
Salpas et al. (1987a) provided analyses of an anorthositic clast and six feldspathic granulites obtained from the 1984 sawing (Table 8; Fig. 23). The anorthosite (,350) is similar to other ferroan anorthosites except that its rare earth elements and transition metals are slightly higher than typical; however, the sample mass was only 17 mg. The clast has a positive Eu anomaly and on the basis of the low upper limits on the Ni and Ir abundances, the sample would appear to be uncontaminated with meteoritic material.
The six granulites show a range in alumina from 22.1 to 27.2%, with corresponding variations in Fe, Mg, Sc, and other transition metals. They appear to represent distinct sources, because they show a range in Mg' consistent with their mineralogy. All are intermediate in major element compositions between ferroan anorthosites and Mg-suite troctolites. Their rare earth element abundances are similar, with fairly flat patterns and mainly small Eu anomalies. All show elevated Ni, Au, and Ir abundances indicative of substantial meteoritic contamination; these elements show abundances higher than in A 16 feldspathic granulites.

STABLE ISOTOPES

Oxygen isotope ratios were measured by Clayton and Mayeda (1975a, b) and Mayeda et al. (1975) for a friable matrix sample, both bulk and mineral separates, and for mineral separates from a KREEPy basalt fragment. The bulk breccia, for which delta $^{18}0$ (5.80) and delta $^{17}0$ (2.94) were measured, falls on the earth-Moon mass fractionation line (Clayton and Mayeda,1975a,b). A second split of the matrix gave delta $^{18}0$ of

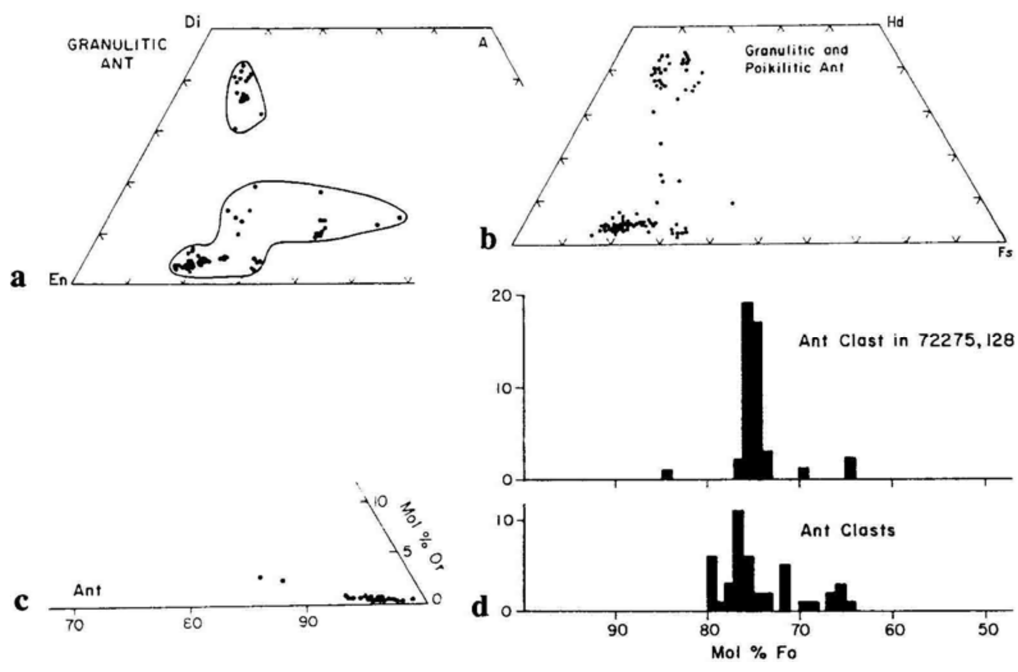

Figure 17. Compositions of silicate mineral phases in feldspathic (mainly feldspathic granulite) breccia clasts in 72275 (and including data for some similar clasts in 72255). a) pyroxenes, Stoeser et al. (1974a). b) pyroxenes, Ryder et al. (19756), c) plagioclases, Ryder et al. (1975b). d) olivines, Ryder et al. (1975b).

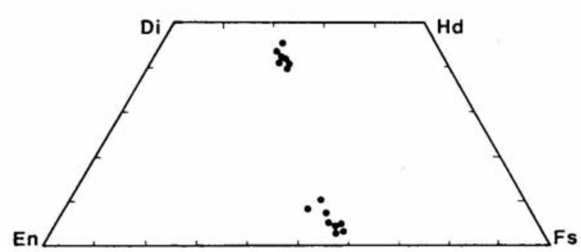

Figure 18: Compositions of pyroxenes in a cataclastic ferroan anorthosite clast (thin section 72275,9018). Salpas et al. (1987x).

5.40, with plagioclase at 5.61 and pyroxene at 5.20. The basalt separates gave plagioclase 5.69 and pyroxene 5.35 (Mayeda et a1.,1975). The matrix values are at the low end of highlands rocks.

RADIOGENIC ISOTOPES AND GEOCHRONOLOGY

Light gray friable matrix: Compston et al. (1975) analyzed a 16.2 mg sample of matrix for Rb and Sr isotopes (Table 9). The data, which are plotted but not specifically discussed by Compston et al. (1975), fall on the mixing line between "gabbroic anorthosites" and micrograntes discussed in the section on 72255. These data are fairly similar to those of the KREEPy basalt, which is probably a component of the sample analyzed. Nyquist et al. (1974a, b) also analyzed a bulk matrix sample for Rb and Sr isotopes (Table 9), with results similar to those of Compston et al. (1975). The Nyquist et al. (1975a,b) data correspond to T_{BABI} and T_{LUNI} model ages of 4.13 and 4.15 Ga respectively (original calculation of 4.22 and 4.24 Ga +/- 0.05 using the old decay constant).

Leich et al. (1975a, b) attempted to date a friable matrix sample using 40Ar-39Ar methods The release diagram (Fig. 24) for this sample (,57) shows an incipient apparent-age plateau that is cut short by a drop-off in the 1000 degree C fractions. The release is broadly similar to that of clast #5 KREEPy basalt (also on Fig. 24). As ,57 is from matrix adjacent to KREEPy basalt clast #4, this matrix sample may be reflecting the pattern for the KREEP basalt. The friable matrix has many components, so a simple, one age release cannot particularly be expected. Leich et al. (1975a, b) interpret the pattern as resulting from truncation of the plateau to two temperature steps from out-gassing of Fe- or Ti-rich (or both) phases, and state that the data are not adequate for chronological interpretation.

Nunes et al. (1974), Nunes and Tatsumoto (1975a), and Tatsumoto et al. (1974) reported U, Th-Pb isotopic data and age parameters for 72275 samples, including the friable matrix (72275,73; Table 10). The Pb data plots within error of Concordia at about 4.25 Ga (see

Table 4: Petrographic features of 6 feldspathic granulite clasts in 72275 (Salpas et al., 1987a).

INAA/PM:	439/495	355/502	351/9019	397/9021	433/493	none/480
Texture	c-g	g-c	c-g	g-c	c	g-c
Plagioclase						
Mode	46%	66%	59%	57%	76%	52%
Size	< 10-350 μm	< 10-400 μm	< 10-650 μm	< 10-500 μm	< 10-340 μm	< 10-500 μm
An	95.9-97.1	94.1-95.3	95.8-96.4	95.4-96.3	94.8-95.8	95.2-97.3
Pyroxene						
Mode	50%	31%	35%	40%	20%	44%
Size	< 10 μm	< 10 μm	< 10 μm	< 10 μm	< 10 μm	< 10 μm
	na	na	na	na	na	na
Olivine						
Mode	1%	3%	5%	1%	2%	2%
Size	40-175 μm	50-150 μm	80-450 μm	100-150 μm	30-45 μm	45-500 μm
Fo	80-82	71-77	63-64	76-77	75-76	75-77
Fe metal						
Mode	3%	< 1%	1%	1%	2%	2%
Size	< 10 μm	< 10 μm	< 10 μm	< 10 μm	< 10 μm	< 10-20 μm
	na	na	na	na	na	see text

c = cataclastic; g = granulitic; na = not analyzed. Analyzed compositions are for mineral fragments and do not include groundmass minerals that were generally too small for accurate analysis.

Table 5a: Chemical analyses of friable matrix samples from 72275.

	,57	,57	,101	,57	,57	,52	,73	,73	,110	,66	
Split							1	2			Split
wt %											wt %
SiO_2	48.6	48	46.2								SiO_2
TiO_2	1.2	0.8	0.94								TiO_2
Al_2O_3	14.7	17.9	18.4								Al_2O_3
Cr_2O_3	0.444	0.25	0.383								Cr_2O_3
FeO	(a)13.8	9.9	(b)11.9								FeO
MnO	0.226	0.12	0.182								MnO
MgO	9.52	11.0	9.9								MgO
CaO	11.0	11.0	11.7		11.8						CaO
Na_2O	0.480	0.40	0.49								Na_2O
K_2O	0.276	0.22	0.265		0.30						K_2O
P_2O_5											P_2O_5
ppm											ppm
Sc	44.7	39	30.6								Sc
V											V
Co	30.4	27	226								Co
Ni	75		950	97							Ni
Rb				5.9		8.2					Rb
Sr					112	115.3					Sr
Y											Y
Zr					667						Zr
Nb											Nb
Hf	16.5	14.0	14.1								Hf
Ba					346						Ba
Th	6.1		5.6				5.962	6.285			Th
U				1.500	1.52		1.561	1.672	1.6		U
Cs				0.255							Cs
Ta	1.7		1.6				3.096	3.451			Ta
Pb											Pb
La	50.5	47	38								La
Ce	130	150	104								Ce
Pr											Pr
Nd											Nd
Sm	24.6	24.5	19.1								Sm
Eu	1.57	1.67	1.46								Eu
Gd											Gd
Tb	3.9	6.1	3.4								Tb
Dy											Dy
Ho											Ho
Er											Er
Tm											Tm
Yb	15.0	15.1	13.3								Yb
Lu	2.01	2.21	1.74								Lu
Li									12		Li
Be											Be
B											B
C											C
N											N
S											S
F									117		F
Cl									29.6		Cl
Br				0.048					0.124		Br
Cu											Cu
Zn				2.7							Zn
ppb											ppb
Au				0.82							Au
Ir				2.26							Ir
I									3.3		I
At											At
Ga											Ga
Ge				406							Ge
As											As
Se				34							Se
Mo											Mo
Tc											Tc
Ru										≤3	Ru
Rh											Rh
Pd											Pd
Ag				0.74							Ag
Cd				13							Cd
In											In
Sn											Sn
Sb				1.17							Sb
Te				4.14							Te
W											W
Re				0.225							Re
Os										1.5	Os
Pt											Pt
Hg											Hg
Tl				0.71							Tl
Bi				0.11							Bi
	(1)	(1)	(1)	(2)	(3)	(4)	(5)	(5)	(6)	(6)	

References and methods:
(1) Blanchard et al (1975); AAS; INAA Cl(1) Cl(2)
(2) Morgan et al (1974, 1975); RNAA Cl(1) Cl(2)
(3) Leich et al (1975); Irradiation/MS (K, Ca) others, ID/MS C(2)
(4) Compston et al (1975); ID/MS
(5) Nunes et al (1974) Tatsumoto et al. (1974) Cl(1); ID/MS Tab et al (1974).
(6) Jovanovic & Reed (1974, a, b 1975) Cl(2); RNAA

(a) AAS; INAA = 14.2%
(b) AAS; INAA = 11.8%
(c) from Wiesmann and Hubbard et al. (1974) gives 0.288%)

Table 5a: Continued.

Split	,90	,2	,2	,71	,2	,108
wt %						
SiO_2	47.31		47.54			48.5
TiO_2	0.94		0.91			0.95
Al_2O_3	16.90		17.01			17.2
Cr_2O_3	0.34	0.343	0.36			0.39
FeO	12.45		11.58			11.4
MnO	0.19		0.18			
MgO	9.47		9.35			8.94
CaO	11.72		11.71			11.6
Na_2O	0.35	0.36	0.38			0.40
K_2O	0.22	(c)0.276	0.28			0.25
P_2O_5	0.38		0.35			
ppm						
Sc	40					48
V	75					115
Co	37					33
Ni	127		67			120
Rb	4.6	8.97	8.7			6.1
Sr	135	122.7	121			
Y	88		129			160
Zr	545	605	613			485
Nb	24		32			31
Hf		14.6				13.3
Ba	330	350				440
Th		5.29				6.70
U		1.56				1.70
Cs						0.31
Ta						
Pb	<2					4.0
La	35	41.0				42.9
Ce		106				114
Pr						17
Nd		67.4				73
Sm		18.8				21.3
Eu		1.49				1.57
Gd		23.4				24.4
Tb						3.86
Dy		23.2				24.4
Ho						5.85
Er		13.7				15.8
Tm						2.1
Yb	9.2	11.6				13.9
Lu		1.71				2.1
Li	13	13.8				
Be	3.8					
B						
C				23		
N				45		
S			800	860	890	
F						
Cl						
Br						
Cu	5.4					5
Zn	<4		3			
ppb						
Au						
Ir						
I						
At						
Ga	3200					
Ge						
As						
Se						
Mo						
Tc						
Ru						
Rh						
Pd						
Ag						
Cd						
In						
Sn						
Sb						
Te						
W						
Re						
Os						
Pt						
Hg						
Tl						
Bi						
	(7)	(8)	(9)	(10)	(11)	(12)

References and methods:
(7) Rose et al (1974); XRF, OE; etc.
(8) Hubbard et al (1974) Wiesmann & Hubbard (1975); AAS, ID/MS. Nyquist et al (1974) a,b.
(9) LSPET (1973 a,b); XRF
(10) Moore et al (1974, a, b), Moore & Lewis (1976); combustion
(11) Gibson and Moore (1974 a, b)
(12) Taylor et al (1974); SSMS/microprobe.

Table 5b: Chemical analyses of friable matrix samples from 72275.
All data by neutron activation. Salpas et at (1987b).

	413	417	423
Major Elements (wt %)			
FeO	14.50	15.05	15.16
CaO	10.1	10.3	12.1
Na_2O	0.42	0.38	0.37
Trace Elements (ppm)			
Sc	45.7	48.6	49.8
V‡	na	na	na
Cr	3062	3088	3255
Mn‡	na	na	na
Co	31.3	33.3	35.3
Ni	12	55	<110
Rb	13	12	14
Sr	138	93	<160
Cs	0.37	0.40	0.44
Ba	370	400	400
La	47.9	50.2	52.3
Ce	129	133	139
Nd	80	81	85
Sm	22.2	23.5	25.5
Eu	1.62	1.66	1.68
Tb	4.59	4.97	5.10
Yb	13.5	13.9	13.1
Lu	1.73	1.80	1.90
Zr	600	765	700
Hf	16.4	17.2	17.9
Ta	1.55	1.66	1.58
Th	5.52	5.46	6.01
U	1.30	1.58	1.26
Ir†	nd	nd	nd
Au(ppb)	<5	<7	<6
weight (mg	105.10	123.88	23.59

*SiO_2 by difference.
†nd = not detected (Ir detection limit = 2 ppb).
‡na = not analyzed.

section on 72215, Fig. 10). The high U and Th abundances in 72275,73 suggest that it contains a high proportion of A 17 KREEPy basalt.

A 17 KREEPy basalts:
Compston et at (1975 and in Cl 2, 1974) reported Rb-Sr isotopic data for separates of a KREEPy basalt sample, 72275,171, described as a basalt of medium grain size. It was probably a subsample of clast #4; it certainly was not clast #5. The data conform to an internal isochron age of 3.93 +/- 0.04 Ga with an initial $^{87}Sr/^{86}Sr$ of 0.69957 +/-14 (Table 11a; Fig. 25a). All the splits fit the isochron within analytical uncertainty. Compston et at (1975) interpret the age to be that of original lava crystallization, before incorporation into the breccia.

Rb-Sr isotopic data for separates of a split, 543 of the KREEPy basalt were reported by Shih et at (1992) (Table lib). The data yield an isochron age of 4.09 t 0.08 Ga (new Rb decay constants) and initial $^{87}Sr/^{86}Sr$ of 0.69960 ± 0.00012 (Fig. 25b). A subset of whole-rock and 3 separates yields a good linear relationship corresponding with 4.06 f 0.01 Ga. The age is older than and resolved from that calculated from the data of Compston et at (1975). The initial isotopic ratios agree within uncertainty. Shih et at (1992) infer separate but similar volcanic events. The data scatter around the best fit line and suggest some disturbance. The model age (TLuni) for,543 is similar to that of other KREEP materials at about 4.3 Ga.

Shih et at (1992) also reported Sm-Nd isotopic data for separates of split,543. (Table 11c). The data correspond with an age of 4.08 t 0.07 Ga (Fig. 25c), with all points fitting within uncertainty of the Rb-Sr age (whichever Rb decay constant is used, and whether the whole Sr data set or the subset is used). Shih et at (1992) prefer the old Rb decay constant and suggest that the basalt is 4.08 Ga old, and significantly older than Apollo 15 KREEP basalts. The initial (Epsilon) Nd value relative to CHUR is slightly negative at -0.61 f 0.23, suggesting derivation from a non-chondritic, low Sm/Nd (light rare earth enriched) source.

Leich et al (1975) provided ^{4O}Ar-39Ar data for 72275, 91, a subsample of the clast #5 KREEPy basalt (Fig. 24). They found the data inadequate for chronological interpretation, mainly because of the drop-off at 1000 degrees C, similar to the friable matrix sample. The highest ages indicated correspond roughly with the Rb-Sr isochron age.

Nunes and Tatsumoto (1975) provided U,Th-Pb isotopic data and age parameters for 72275,170, the same clast analyzed by Compston et al. (1975) (Table 12). The data lie within analytical uncertainty of an approximately 3.9 - 4.4 Ga discordia line; varied calculated single-stage ages are in the 4.05 - 4. 10 Ga range. However, if the crystallization age is 3.93 Ga (Rb-Sr), then the older $207p_b/206_{Pb}$ age (4.1 Ga) must result from addition of Pb to the sample. This is presumably from the boulder matrix.

Dark impact melt breccias:
L.eich et at (1975a) provided ^{40}Ar-^{39}Ar data for the dark melt breccia clast #2, split 72275,83 (Fig. 26a). The drop-off of the intermediate plateau precludes an age determination, although an age of about 3.9 +/- 0.1 Ga is surely suggested by the data.

Table 5c: Chemical analyses of dark melt breccia {clast #2} in 72275.

Split	,83	,83	,83	,161
wt %				
SiO_2	46			
TiO_2	0.8			
Al_2O_3	19.7			
Cr_2O_3	0.24			
FeO	9.9			
MnO	0.111			
MgO	10.4			
CaO	12.0		11.9	
Na_2O	0.30			
K_2O	0.25		0.28	
P_2O_5				0.6
ppm				
Sc	28			
V				
Co	30			
Ni		147		
Rb		5.4		
Sr				
Y				
Zr				
Nb				
Hf	13.7			
Ba				
Th				
U		1.840		2.7
Cs		0.255		
Ta				
Pb				
La	41			
Ce	112			
Pr				
Nd				
Sm	18.7			
Eu	1.50			
Gd				
Tb	3.8			
Dy				
Ho				
Er				
Tm				
Yb	12.1			
Lu	1.82			
Li				8
Be				
B				
C				
N				
S				
F				77
Cl				28.9
Br		0.095		0.395
Cu				
Zn		2.4		
ppb				
Au		1.30		
Ir		3.44		
I				1.5
At				
Ga				
Ge		178		
As				
Se		52		
Mo				
Tc				
Ru				6.8
Rh				
Pd				
Ag		0.56		
Cd		26		
In				
Sn				
Sb		1.06		
Te		2.74		
W				
Re		0.334		
Os				10
Pt				
Hg				
Tl		0.62		
Bi		0.12		
	(1)	(2)	(3)	(4)

References and methods:
(1) Blanchard et al (1975); AAS, INAA C(1) C(2)
(2) Morgan et al (1974, 1975); RNAA Cl(1) Cl(2)
(3) Leich et al (1975); Irradiation/MS Cl(2)
(4) Jovanovic & Reed (1975 a,b,c,d); RNAA Cl(2)

Table 6a: Chemical analyses of A 17 KREEPy basalts made from 1973 slab allocations, plus, 543

Split	,91	,91	,91	,171 (1)	,171 (2)	,170	,543	Split
wt %								wt %
SiO_2	48							SiO_2
TiO_2	1.4							TiO_2
Al_2O_3	13.5							Al_2O_3
Cr_2O_3	0.46							Cr_2O_3
FeO	15							FeO
MnO	0.156							MnO
MgO	10.0							MgO
CaO	10.5		11.6					CaO
Na_2O	0.29							Na_2O
K_2O	0.25		0.29					K_2O
P_2O_5								P_2O_5
ppm								ppm
Sc	61							Sc
V								V
Co	37							Co
Ni		43						Ni
Rb		8.0		6.34	7.53		7.23	Rb
Sr			92	81.1	91.8		89.20	Sr
Y								Y
Zr			625					Zr
Nb								Nb
Hf	18							Hf
Ba			355					Ba
Th						6.255		Th
U		1.500	1.53			1.635		U
Cs		0.355						Cs
Ta								Ta
Pb						3.049		Pb
La	48							La
Ce	131							Ce
Pr								Pr
Nd							65.15	Nd
Sm	23						18.13	Sm
Eu	1.58							Eu
Gd								Gd
Tb	4.5							Tb
Dy								Dy
Ho								Ho
Er								Er
Tm								Tm
Yb	11.9							Yb
Lu	1.75							Lu
Li								Li
Be								Be
B								B
C								C
N								N
S								S
F								F
Cl								Cl
Br		0.044						Br
Cu								Cu
Zn		2.7						Zn
ppb								ppb
Au		0.045						Au
Ir		0.023						Ir
I								I
At								At
Ga								Ga
Ge		1290						Ge
As								As
Se		230						Se
Mo								Mo
Tc								Tc
Ru								Ru
Rh								Rh
Pd								Pd
Ag		0.58						Ag
Cd		8.3						Cd
In								In
Sn								Sn
Sb		2.87						Sb
Te		7.8						Te
W								W
Re		0.0066						Re
Os								Os
Pt								Pt
Hg								Hg
Tl		0.58						Tl
Bi		0.14						Bi
	(1)	(2)	(3)	(4)	(4)	(5)	(6)	

References and methods:
(1) Blanchard et al (1975); AAS; INAA Cl(1) Cl(2)
(2) Morgan et al (1974, 1975); RNAA Cl(1) Cl(2)
(3) Leich et al (1975); Irradiation/MS (K, Ca) other: ID/MS
(4) Compston et al (1975); ID/MS Cl(2)
(5) Nunes & Tatsumoto (1975); ID/MS
(6) Shih et al. (1992)

Notes:
,91 is clast #5
,170 and ,171 are probably clast #4.

Table 6b: Chemical analyses of A 17 KREEPY basalts and pristine basaltic breccias made from 1984 slab allocations. All data from neutron activation; SiO_2 where given is by difference.
(Salpas *et al*., 1987b).

	357	359	365A	365B	415	427A	427B	427C	431
				Major Elements (wt %)					
SiO_2*	51.3	50.7	50.1	51.0	48.6	50.1	48.3	47.9	49.6
TiO_2	1.54	1.03	1.20	1.29	1.48	1.01	1.20	1.22	1.25
Al_2O_3	14.5	13.7	15.9	13.6	13.3	12.5	12.5	13.4	13.1
FeO	13.9	14.0	12.5	13.8	15.5	16.1	16.5	17.0	15.9
MgO	6.8	9.6	9.0	8.9	9.3	10.4	11.4	10.8	9.0
CaO	10.8	10.4	10.5	10.8	11.1	9.2	9.5	9.0	10.3
Na_2O	0.510	0.401	0.474	0.409	0.473	0.442	0.415	0.438	0.408
				Trace Elements (ppm)					
Sc	51.9	47.4	38.7	51.1	48.9	46.5	45.5	47.4	51.4
V	97	134	89	109	118	125	135	144	132
Cr	1960	3270	2460	2670	3275	3780	4420	4850	3790
Mn	1340	1670	1500	1630	1770	1820	1700	1940	1670
Co	30.9	34.5	28.6	32.4	33.2	37.8	46.4	43.7	36.6
Ni	<80	52	51	39	42	76	112	80	64
Rb	12	15	11	21	10	10	12	16	16
Sr	92	91	83	78	90	124	98	90	105
Cs	0.40	0.35	0.46	0.94	0.46	0.43	0.30	0.46	0.41
Ba	500	330	440	425	430	360	365	390	380
La	61.7	39.7	47.1	53.2	51.4	44.7	46.2	51.1	46.4
Ce	155	102	122	138	139	114	121	130	128
Nd	108	66	79	87	83	78	75	85	73
Sm	28.9	18.3	22.2	24.9	24.0	20.7	22.3	24.2	17.8
Eu	1.87	1.42	1.62	1.72	1.69	1.50	1.45	1.59	1.51
Tb	5.82	3.92	4.48	4.88	4.06	4.48	4.31	5.15	4.70
Yb	15.5	11.0	13.2	14.3	14.3	12.3	12.4	12.5	13.3
Lu	2.18	1.49	1.77	1.94	1.86	1.66	1.67	1.88	1.72
Zr	610	450	600	620	640	520	540	490	600
Hf	20.5	13.5	15.9	17.9	18.0	15.3	15.9	17.5	16.2
Ta	1.90	1.20	1.45	1.58	1.62	1.33	1.37	1.56	1.48
Th	6.73	4.46	5.97	6.10	5.84	4.72	5.25	5.60	5.10
U	1.95	1.22	1.40	1.52	1.58	1.30	1.45	1.33	1.30
Ir†	nd	nd	nd	nd	nd	nd	nd	nd	nd
Au (ppb)	<4	<4	<4	<4	<5	<4	<4	<4	<2
weight (mg)	8.48	84.42	33.67	48.40	76.00	35.81	29.50	5.34	64.64

	347	363A	363B	371	385	387	389	391	393	411	419A	443	449	453	460
					Major Elements (wt %)									*Major Elements (wt %)*	
FeO	15.5	14.7	14.8	14.56	15.18	13.64	15.77			14.61	14.85	13.50	12.37	14.92	14.88
CaO	9.7	10.4	11.0	11.4	9.1	10.4	9.1	10.0	10.3	9.4	9.7	11.2	10.1	12.0	10.0
Na_2O	0.440	0.465	0.473	0.34	0.35	0.412	0.394	0.431	0.408	0.47	0.37	0.477	0.419	0.35	0.33
					Trace Elements (ppm)									*Trace Elements (ppm)*	
Sc	48.2	46.6	51.0	49.4	50.0	50.9	49.0	43.0	49.9	50.1	48.9	49.0	36.2	49.5	49.2
V‡	na	na	na	na	na	na	na	na	na	na	na	na	na	na	na
Cr	3120	2990	2240	3056	3170	3825	3280	3130	3605	3120	3290	3263	2580	2940	3550
Mn‡	na	na	na	na	na	na	na	na	na	na	na	na	na	na	na
Co	32.4	31.4	30.1	32.5	35.1	36.3	35.1	32.4	38.7	32.4	32.6	33.7	28.6	33.1	37.3
Ni	45	54	70	35	50	46	54	62	60	<100	62	49	100	60	76
Rb	9	10	18	16	14	14	15	12	11	8	13	18	10	18	13
Sr	60	104	77	90	93	60	93	58	130	70	63	100	76	60	70
Cs	0.37	0.44	0.47	0.48	0.55	0.43	0.53	0.30	0.35	0.37	0.51	0.60	0.43	0.47	0.40
Ba	400	425	440	400	440	360	360	360	325	430	400	420	360	400	400
La	50.6	49.4	56.7	50.4	52.5	44.9	45.3	45.9	41.3	51.7	49.5	50.8	43.8	53.2	49.7
Ce	128	128	148	135	140	122	123	125	114	138	132	138	116	142	134
Nd	85	88	94	81	92	69	73	78	63	91	85	85	71	84	90
Sm	23.3	23.3	26.7	23.3	23.8	21.2	20.9	20.9	20.8	23.4	22.7	23.6	19.6	25.7	22.9
Eu	1.60	1.59	1.76	1.68	1.62	1.54	1.53	1.56	1.63	1.67	1.61	1.68	1.54	1.70	1.60
Tb	4.59	4.54	5.15	4.86	4.90	4.99	4.56	4.65	4.21	4.94	4.83	4.97	4.27	5.22	4.94
Yb	13.6	13.3	14.9	14.0	13.8	12.7	12.4	12.7	10.8	13.8	13.2	14.2	12.3	13.5	13.5
Lu	1.85	1.80	2.00	1.81	1.83	1.64	1.65	1.69	1.43	1.83	1.77	1.86	1.64	1.95	1.77
Zr	600	570	650	650	800	570	680	640	540	750	750	670	620	790	600
Hf	17.0	16.5	19.0	17.5	17.4	15.5	15.5	15.2	14.6	17.3	16.6	17.8	14.7	18.6	16.8
Ta	1.49	1.44	1.70	1.54	1.62	1.41	1.45	1.46	1.17	1.61	1.56	1.66	1.49	1.65	1.56
Th	5.85	5.75	6.79	5.72	5.98	4.91	5.29	5.68	2.96	6.16	5.68	5.94	5.61	6.20	5.53
U	1.42	1.54	1.60	1.28	1.30	1.21	1.35	1.30	0.80	1.65	0.91	1.40	1.08	1.35	1.18
Ir†	nd	nd	nd	nd	nd	nd	nd	nd	nd	nd	nd	nd	nd	nd	nd
Au(ppb)	<4	<4	<4	<7	<7	<7	<3	<4	<3	:7	<6	<4	<5	<6	<10
weight (mg)	66.04	32.39	22.34	110.26	58.10	84.40	45.60	49.74	70.65	49.62	55.18	74.36	61.78	31.43	61.48

*SiO_2 by difference.
†nd = not detected (Ir detection limit = 2 ppb).
‡na = not analyzed.

Table 7: Chemistry of components of clast #1 (Marble Cake clast) of 72275.

	White (An Bx)			Dark (BC Bx)						
	,76	,117	,76	,80	,166(,62)a	,81	,80	,80	,168(,62)	
Split										Split
wt %										wt %
SiO_2	47			47	47					SiO_2
TiO_2	1.8			1.8	1.1					TiO_2
Al_2O_3	23.5			17.9	18.2					Al_2O_3
Cr_2O_3	0.20			0.46	0.27					Cr_2O_3
FeO	7.4			10.3	(b)10.9					FeO
MnO	0.077			0.104	0.167					MnO
MgO	5.24			9.43	9.14					MgO
CaO	14.2		14.6	11.7	11.2		8.5			CaO
Na_2O	0.36			0.39	0.63					Na_2O
K_2O	0.32		0.40	0.47	0.49		0.41			K_2O
P_2O_5										P_2O_5
ppm										ppm
Sc	25			34	26.3					Sc
V										V
Co	18.7			28	22.5					Co
Ni					130			122	121	Ni
Rb								11.3	13.0	Rb
Sr			171				151			Sr
Y										Y
Zr			479				908			Zr
Nb										Nb
Hf	14			19.8	25.1					Hf
Ba			361				683			Ba
Th					12.8	13.21				Th
U		0.670	1.60			3.500	3.19	3.100	3.280	U
Cs								0.47	0.50	Cs
Ta					3.5					Ta
Pb		1.410				7.878				Pb
La	48			78	78					La
Ce	131			213	206					Ce
Pr										Pr
Nd										Nd
Sm	22.5			36	36					Sm
Eu	1.81			2.14	2.10					Eu
Gd										Gd
Tb	4.7			7.7	7.7					Tb
Dy										Dy
Ho										Ho
Er										Er
Tm										Tm
Yb	13.9			24	25.4					Yb
Lu	2.04			3.5	3.5					Lu
Li										Li
Be										Be
B										B
C										C
N										N
S										S
F										F
Cl										Cl
Br								0.290	0.283	Br
Cu										Cu
Zn								2.8	11.7	Zn
ppb										ppb
Au								1.16	1.84	Au
Ir								2.54	3.91	Ir
I										I
At										At
Ga										Ga
Ge								137		Ge
As										As
Se								63	72	Se
Mo										Mo
Tc										Tc
Ru										Ru
Rh										Rh
Pd										Pd
Ag								0.93	1.46	Ag
Cd								15	13.9	Cd
In										In
Sn										Sn
Sb								0.94	1.42	Sb
Te								3.46	1.9	Te
W										W
Re								0.233	0.330	Re
Os										Os
Pt										Pt
Hg										Hg
Tl								0.71	1.40	Tl
Bi								0.14	0.59	Bi
	(1)	(2)	(3)	(1)	(1)	(2)	(3)	(4)	(4)	

References and methods:
(1) Blanchard et al (1975); AAS, INAA Cl(1) Cl(2)
(2) Nunes et al (1974); Tatsumoto et al (1974); ID/MS Cl(1)
(3) Leich et al (1975); Irradiation, MS (K,Ca) and MS/ID (others) Cl(2)
(4) Morgan et al (1974, 1975); RNAA and Higuchi and Moyen (1975) Cl(1) Cl(2)

Notes:
(a) Dark separate from interior white.
(b) AAS; INAA = 10.8%

Table 8: Partial analyses of six feldspathic granulites and one anorthosite (FAN) from 72275, obtained by neutron activation. Salpas et al. (1987a).

	Granulites						FAN
	351A	351B	355A	397	433	439	350
	Major Elements (wt %)						
TiO_2	0.31	0.32	0.29	0.22	0.15	0.32	na
Al_2O_3	22.1	23.1	27.2	26.2	24.6	26.3	na
FeO	8.87	7.83	4.85	5.71	5.10	4.95	0.485
MgO	11.5	9.9	7.6	7.9	8.0	9.7	na
CaO	11.9	12.6	14.8	14.8	14.2	14.5	19.2
Na_2O	0.307	0.316	0.349	0.353	0.362	0.350	0.456
	Trace Elements (ppm)						
Sc	14.97	12.92	8.13	7.81	8.24	7.12	1.12
V	69	65	19	20	24	25	na
Cr	2414	1646	810	842	881	846	46.6
Mn	934	792	489	499	481	462	na
Co	35.1	34.1	27.0	39.3	30.6	52.0	0.440
Ni	250	290	340	455	422	540	< 7
Sr	124	129	157	160	160	163	205
Cs	0.124	0.118	0.164	0.19	0.23	0.10	0.016
Ba	58	55	70	72	87	62	40
La	4.86	3.56	4.04	3.66	4.72	3.76	0.567
Ce	10.9	8.62	9.87	10.1	12.6	10.5	1.48
Nd	7.0	5.5	5.6	5.7	6.2	5.0	< 2.5
Sm	2.04	1.60	1.82	1.56	1.93	1.67	0.228
Eu	0.698	0.713	0.864	0.835	0.860	0.870	0.928
Tb	0.473	0.410	0.456	0.375	0.49	0.381	0.045
Yb	2.05	1.66	1.67	1.69	2.06	1.55	0.125
Lu	0.302	0.242	0.251	0.238	0.292	0.230	0.020
Hf	1.67	1.24	1.46	1.46	1.98	1.22	0.133
Ta	0.266	0.199	0.233	0.302	0.309	0.190	0.015
Th	1.81	1.38	1.18	1.17	2.06	1.02	0.047
U	0.39	0.27	0.30	0.34	0.37	0.19	0.020
Ir (ppb)	9.6	11.3	13.0	16.4	14.0	22.2	nd
Au (ppb)	3.4	3.6	5.0	6.8	6.5	4.3	< 0.8

na = not analyzed.
nd = not detected (Ir detection limit = 2 ppb).

Table 9: Rb-Sr isotopic data for 72275 friable matrix samples.

Sample	Mass mg	Rb ppm	Sr ppm	$^{87}Rb/^{87}Sr$	$^{87}Sr/^{87}Sr$ +/-s.e.
a) ,52	16.2	8.20	115.3	0.2053	0.71139 3
b) ,2	52.8	8.97	122.7	0.2115	0.71188 3

a) Compston et al. (1975) b) Nyquist et al. (1974a,b).

Table 10: U,T6-Pb data and age parameters for 72275 friable matrix and clast #1 (Marble Cake) samples.
Nunes *et al*. (1974).

Sample	Weight (mg)	Concentrations (ppm) U	Th	Pb	$^{232}Th/^{238}U$	$^{238}U/^{204}Pb$
Boulder 1, Station 2						
72275,73 matrix	131.8	1.561	5.962	3.096	3.95	4,284
	150.0	1.672	6.285	3.451	3.89	4,712
72275,81 clast # 1 black rind	31.7	3.500	13.21	7.878	3.90	2.493
72275,117 clast # 1 white interior	50.7	0.670	—	1.410	—	2.445

Sample	Weight (mg)	Run	Observed ratios† $^{206}Pb/^{204}Pb$	$^{207}Pb/^{204}Pb$	$^{208}Pb/^{204}Pb$	Corrected for analytical blank‡ $^{206}Pb/^{204}Pb$	$^{207}Pb/^{207}Pb$	$^{208}Pb/^{204}Pb$	$^{207}Pb/^{206}Pb$	$^{208}Pb/^{206}Pb$
Boulder 1, Station 2										
72275,73 matrix	162.0	P	1,097	537.1	1,090	1,225	599.3	1,218	0.4893	0.9945
	131.8	C1*	2,715	1,308	—	3,961	1,905	—	0.4811	—
		C2*	3,220	1,545	—	4,556	2,183	—	0.4792	—
72275,81 clast # 1 black rind	53.3	P	1,578	959.2	1,532	1,937	1,176	1,880	0.6072	0.9705
	31.7	C*	1,688	1,000	—	2,521	1,492	—	0.5918	—
72275,117 clast # 1 white interior	83.3	P	902.2	520.8	860.4	1,423	818.2	1,347	0.5752	0.9472
	50.7	C*	920.4	533.3	—	2,361	1,360	—	0.5761	—

Sample	Run	Corrected for blank and primordial Pb $^{206}Pb/^{238}U$	$^{207}Pb/^{235}U$	$^{207}Pb/^{206}Pb$	$^{208}Pb/^{232}Th$	Single-stage ages in m.y. $^{206}Pb/^{238}U$	$^{207}Pb/^{235}U$	$^{207}Pb/^{206}Pb$	$^{208}Pb/^{232}Th$
72275,73 matrix	C1P	0.9175	61.26	0.4845	0.2274	4,236	4,250	4,256	4,198
	C1	0.9223	60.95	0.4796	—	4,252	4,245	4,241	—
72275,81 clast # 1 black rind	C1P	1.006	83.88	0.6048	0.2478	4,531	4,568	4,585	4,535
	C1	1.008	81.90	0.5899	—	4,534	4,544	4,548	—
72275,117 clast # 1 white interior	C1P	0.9595	75.60	0.5717	—	4,377	4,463	4,502	—
	C1	0.9620	76.09	0.5740	—	4,385	4,469	4,508	—

Table 11a: Rb-Sr data for KREEPY basalt separates.
Compston *et al*. (1975).

Rb, Sr, and $^{87}Sr/^{86}Sr$ analyses for pigeonite basalt 72275,171. Blank levels for these data are 0.035 ng Rb and 0.10 ng Sr. Our mean normalised $^{87}Sr/^{86}Sr$ for the NBS987 reference sample is 0.71028 ± 1 (s.e.)

	Weight (mg)	Rb (ppm)	Sr (total) (ppm)	$^{87}Rb/^{86}Sr$	$^{87}Sr/^{86}Sr$ (±s.e.)[a]
Mesostasis	1.48	18.8	122.9	0.4417	0.72489±6
Plagioclase	1.05	1.68	173.3	0.02799	0.70117±4
Pigeonite	1.93	0.427	5.80	0.2127	0.71124±42
Total-rock (1)	11.3	6.34	81.1	0.2260	0.71262±3
Total-rock (2)	11.9	7.53	91.8	0.2370	0.71307±9

[a] Internal standard error of mean.

Table 11b: Rb-Sr data for KREEPy basalt separates.
Shih *et al* (1992).

Sample	Wt. (mg)	Rb (ppm)	Sr (ppm)	$^{87}Rb/^{86}Sr$ [a]	$^{87}Sr/^{86}Sr$ [a,b]	T_{LUNI} (Ga) [c,d]
WR	11.16	7.323	89.20	0.2375 ±12	0.713690±17	4.31±0.02
Plag	2.10	1.040	184.1	0.01634±12	0.700530±19	
Opx	2.76	0.6779	18.95	0.10350±74	0.705463±25	
Opaques	1.04	28.10	96.95	0.8386 ±49	0.748935±19	
$\rho < 2.75$ [e]	3.50	6.364	199.3	0.09241±48	0.705221±10	
$\rho = 3.3–3.55$	6.94	3.250	21.25	0.4424 ±23	0.725513±29	
$\rho > 3.55$	2.07	2.859	18.68	0.4428 ±24	0.725716±19	
NBS 987 ($n = 13$)					0.710251±28 [f]	

[a] Uncertainties correspond to last figures and are $2\sigma_m$.
[b] Normalized to $^{88}Sr/^{86}Sr = 8.37521$ and $^{87}Sr/^{86}Sr = 0.71025$ for NBS 987.
[c] Calculated for $\lambda(^{87}Rb) = 0.0139\ Ga^{-1}$.
[d] Model age relative to the LUNar Initial $^{87}Sr/^{86}Sr$ (LUNI = 0.69903 of Nyquist et al. [21,25]).
[e] Density in g/cm^3 for all mineral separates obtained using heavy liquids.
[f] Mean value of thirteen measurements made during this investigation; error limits are $2\sigma_n$.

Table 11c: Sm-Nd data for KREEPy basalt separates.
Shih et al. (1992).

Sample	Wt. (mg)	Sm (ppm)	Nd (ppm)	$^{147}Sm/^{144}Nd$ [a]	$^{143}Nd/^{144}Nd$ [a,b]	T_{CHONI} (Ga) [c,d]
WR	11.16	18.13	65.15	0.16830±17	0.511036±12	4.60±0.01
Plag	2.10	1.549	6.160	0.15203±75	–	
Opx	2.76	2.127	6.394	0.20118±29	0.511943±12	
Opaques	1.04	88.47	326.3	0.16398±17	0.510937±13	
$\rho < 2.75$ [e]	3.50	9.926	37.63	0.15951±17	0.510816±12	
$\rho = 3.3–3.55$	6.94	9.118	30.27	0.18219±18	0.511418±12	
$\rho > 3.55$	2.07	10.10	34.71	0.17607±18	0.511257±12	
Ames Nd Standard ($n = 16$)					0.511088±12 [f]	

[a] Uncertainties correspond to last figures and are $2\sigma_m$.
[b] Normalized to $^{146}Nd/^{144}Nd = 0.724140$ and $^{143}Nd/^{144}Nd = 0.511138$ for the Ames Nd metal standard which is equivalent to CIT nNdβ standard of Wasserburg et al. [15].
[c] Calculated for $\lambda(^{147}Sm) = 0.00654\ Ga^{-1}$.
[d] Model age relative to the CHONdritic Initial $^{143}Nd/^{144}Nd$ (CHONI = 0.505893 of Jacobsen and Wasserburg [31]).
[e] Density in g/cm^3 for all mineral separates obtained using heavy liquids.
[f] Mean value of sixteen Nd standard measurements made during this investigation; ~ 325 ng of Nd standard were used for each measurement; error limits are $2\sigma_p$, as reported in [14].

Table 12: U, Th-Pb data and age parameters for 72275 KREEPy basalt (probably clast #4).
Nunes and Tatsumoto (1975a).

Sample	Description	Run	Weight (mg)	Concentrations U	Th	Pb	$^{232}Th/^{238}U$	$^{238}U/^{204}Pb$
72275,170	Pigeonite basalt clast (PB)	C1	38.6	1.635	6.255	3.047	3.95	3045

Sample	Description	Run	Weight (mg)	Observed Ratios[c] $^{206}Pb/^{204}Pb$	$^{207}Pb/^{204}Pb$	$^{208}Pb/^{204}Pb$	Corrected for Analytical Blank[b] $^{206}Pb/^{204}Pb$	$^{207}Pb/^{204}Pb$	$^{208}Pb/^{204}Pb$	$^{207}Pb/^{206}Pb$	$^{208}Pb/^{206}Pb$
72275,170	Pigeonite basalt clast (PB)	P	38.9	2360	1079	2387	(34287)	(15592)	(34420)	0.4547	1.0038
		C1	38.6	1299	597.2	–	2672	1220	–	0.4568	–

P=composition run; C=concentration run; (GCBx)=gray competent breccia; (PB)=pigeonite basalt.
[a] Totally spiked runs from solid sample splits; other runs were obtained from samples which were divided from solution.
[b] Pb blanks ranged from 1.4 to 2.1 ng for the solution aliquoted data and were 1.05 ng for the totally spiked data.
[c] Raw data corrected for mass discrimination of 0.15% per mass unit. ^{208}Pb spike contribution subtracted from concentration data.
Data in parantheses subject to extreme error owing to Pb blank uncertainty.
All 72215 samples are competent breccias with colors ranging from black to light-gray.

Sample	Description	Run	Atomic ratios corrected for blank and primordial Pb $^{206}Pb/^{238}U$	$^{207}Pb/^{235}U$	$^{207}Pb/^{206}Pb$	$^{208}Pb/^{232}Th$	Single-stage ages × 10^6 yr $^{206}Pb/^{238}U$	$^{207}Pb/^{235}U$	$^{207}Pb/^{206}Pb$	$^{208}Pb/^{232}Th$
72275,170	Pigeonite basalt clast (PB)	C1P	0.8776	55.00	0.4547	0.2228	4061	4087	4100	4065
		C1	0.8747	54.82	0.4545	–	4051	4084	4100	–

[a] Concentrations determined from totally spiking a separate sample. Concentration and composition splits were divided from perfect solutions prior to spiking for all other analyses.
All 72215 samples are competent breccias with colors ranging from black to light-gray.
P=composition run; C=concentration run; (GCBx)=gray competent breccia; (PB)=pigeonite basalt.

Table 13: Magnetic properties of 72275, 2.
Pearce *et al*. (1974b).

Sample	J_s (emu/g)	X_p (emu/g Oe) $\times 10^6$	X_0 (emu/g Oe) $\times 10^4$	J_{rs}/J_s	H_c (Oe)	H_{rc} (Oe)	Equiv. wt.% Fe°	Equiv. wt.% Fe^{++}	Fe°/Fe^{++}
Noritic rocks									
72275,2	1.12	19.0	3.4	.005	35	—	.51	8.72	.059

Table 14: Magnetic properties (hysteresis parameters) of 72275,67.
Brecher *et al*. (1974).

	72275,67			
Sample (mass, mg)	U(35)		O(104)	
T (°K)	300	160	300	160
J_s (emu/g)	1.28	1.19	.877	.93
J_{rs} ($\times 10^3$ emu/g)	.05	.07	.12	.145
χ_0 ($\times 10^4$ emu/g · Oe)	34.6	48.6	34.3	42.3
χ_p ($\times 10^6$ emu/g · Oe)	6.92	6.62	7.86	7.84
H_c (Oe)	72	105	150	185
m_{Fe° (wt.%)	.59	.54	.40	.43
$f_{Fe^{++}}$ (wt.%)	16.1	12.1	16.0	10.5
Fe°/Fe^{++}	.036	.045	.025	.04
J_{rs}/J_s	.04	.06	.136	.156
J_s/χ_0	1850	1790	1115	1185

Table 15: Native iron determined from J. measurement of 72275 samples.
Banerjee and Swits (1975).

Sample No.	J_s (G-cm^3 g^{-1})	Fe° content (wt. %)	Average
72275,46	3.26	1.52	
72275,47 (1)	4.47	2.08	1.69
72275,47 (2)	2.70	1.26	
72275,56	4.09	1.90	

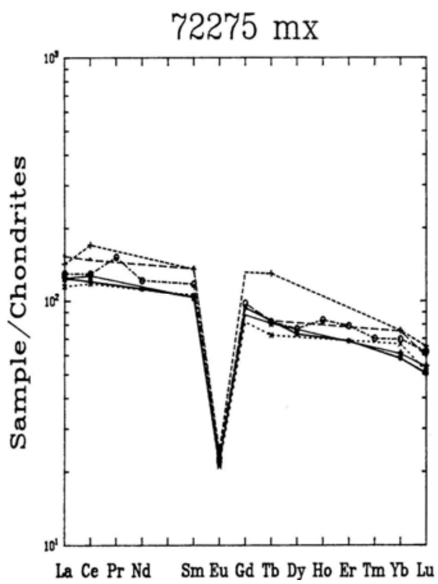

Figure 19a: Abundances of rare earth elements in 72275 friable matrix and dark melt samples. Dark melt breccia clast #2 (,83) is a solid line with +s, and is similar to typical matrix The extremely high REE sample (dashed line with +'s) is a split of,57, and is KREEPy basalt rich. Another split of ,57 (long dashes) has high light but not heavy rare earths. Split .101 is shortest dashes with x's. A larger sample, ,2, is a solid line without added symbols, and,108 is dash-dot with o's. For references, see Tables 5a and 5c.

Clast #1 (Marble Cake):
Leich et al. (1975a) provided ^{40}Ar-39Ar data for the rind (,80) and the interior (76) of the Marble Cake clast (Figs. 26a, b). Like the other samples discussed above, the data for the interior allow no firm chronological interpretation, although again some age around 3.9 Ga for outgassing is suggested by the data. Leich et al. (1975a) however do attach significance to the intermediate plateau for the rind, which gives an age of 3.93 +/- 0.03 Ga (new constants; Fig. 26b).

Nunes et al. (1974) provided U,Th-Pb data for both rind (,81) and interior (117) of the Marble Cake clast (Table 10). The data plot within error of concordia near the 4.5 Ga point.

EXPOSURE AGES AND PARTICLE TRACKS

Leich et al. (1975a) tabulated extensive rare gas isotopic data (He, Ne, Ar, Kr, Xe) for 72275 samples: friable matrix (,57), clast #1 (Marble Cake) core 06) and rind (,80 and,166), and the KREEPy basalt class #5 (,91). Only ,80 shows trapped Ne and Ar components that might be indicative of a small amount of solar wind contamination. $81_{K}r\_{K}r$ exposure ages for four of these samples (KREEPy basalt not included in the exposure tabulations) give a weighted mean of 52.5 m.y., with a 1.3 m.y. standard deviation. This age is about 10 m.y, older than that of samples 72215 and 72255, and indicate different shielding parameters for boulder samples. Exposure ages from ^{38}Ar, ^{83}Kr, and ^{126}Xe are fairly consistent, but from ^{21}Ne and ^{3}1-le are somewhat lower. Exposures calculated from ^{38}Ar-Ca determinations are unreliable (Leich et al., 1975a). Goswami and Hutcheon (1975) studied the particle track record in 72275,44. They found that the extent of shock metamorphism is heterogeneous, and that the sample retained no solar flare tracks. The constituents of the boulder were not exposed to solar radiation prior to the assembly of the boulder and it is not a regolith breccia. Goswami et al. (1977a, b) measured track densities in a whitlockite crystal from 72275. With various assumptions, they calculated a track retention age of 3.98 +0.04/-0.06 Ga for the crystal. This age is the age of last significant heating of the crystal, and therefore an upper limit for the age of compaction of the boulder.

PHYSICAL PROPERTIES

Magnetic properties of 72275 friable matrix samples were reported by Pearce et al. (1974x, b), Brecher et al. (1974), Brecher and Morash (1974), Banerjee et al. (1974a, b), and Banerjee and Swits (1975). The data from Pearce et al. (1974a, b) is given in Table 13, and that from Brecher et al. in Table 14. Native metal contents inferred from is measurements by Banerjee and Swits (1975) are in Table 15, and are substantially higher than those inferred for the matrix sample by Pearce et al. (1974a, b) or Brecher et al. (1974a, b). All measured samples contain much more native metal than do mare samples. Banerjee et al. (1974a, b) and Banerjee and Swits (1975) used samples of known mutual orientations (known within about 20 degrees). They found that the average directions of natural remanent magnetism in all the 72255 and 72275 samples were approximately the same (see diagrams in section on 72255). In an attempt to separate stable primary NRM from unstable secondary NRM, the authors attempted thermal demagnetization, avoiding oxidation; however, it appeared that permanent damage was done to the carriers and the procedure unadvisable. AF-demagnetization showed no zig-zag patterns, and the NRM direction after demagnetization in fields of 80 Oe and greater are stable and primary; however, they differ from those in 72255 by 130 degrees (see diagrams in 72255 section). Banerjee and Swits (1975) presented data for paleointensity, suggesting a field of about 0.19 Oe, lower than those for 72215 and 72255. However, given the problems of obtaining and interpreting magnetic data for lunar samples, neither the directions nor the intensities can be said to have known meanings. Brecher et al. (1974a,b) also tabulated consider-able NRM data for 72275 (Table 16), with extensive discussion. They found a paleointensity similar to that found by Banerjee and Swits (1975). Boulder 1, Station 2 differs greatly in magnetic behavior from the Station 7 Boulder (sample 77135) analyzed in the same study. The paleomagnetic intensities derived appear to depend directly on thermal history, since drastic changes in magnetic mineralogy and character result from even brief heating cycles at 800 degrees C. Housley et al. (1977) in ferromagnetic resonance studies found that 72275,109 had no characteristic FMR intensity.

Adams and Charette (1975) and Charette and Adams (1977) measured the spectral reflectance (0.35 - 2.5 microns) of two samples from 72275 (Fig. 27). 72275,98 is undocumented fines from sawing, and 72275,103 is a surface chip of matrix; both represent general friable matrix. They show the typical absorption bands near 0.9 microns and 1.9 microns that arise from electronic transitions of Fe^{2+} in orthopyroxene, and a broad absorption band near 0.6 microns that is commonly associated with ilmenite.

PROCESSING

The 1973 processing and sawing was described by Marvin (in Cl 1, 1974), and the 1984 processing by Salpas et al. (1985). The sample arrived from the Moon with several pieces dislodged from the friable matrix; some of these could be fitted together, but others remained undocumented. Some were used for thin sections and chemical analyses. A slab (,42) was cut (Figs. 2, 3), and subdivided (Fig. 28). Many allocations were made from this slab. The end pieces remained largely untouched. In 1984 two more slabs were cut parallel to the first one (Fig. 3c, 4, and 5) and allocations, mainly of clasts, were made from them.

Table 16: Magnetic properties of 72275,67. Brecher *et al*. (1974x).

Samples (Mass, g)	72275,67 (.932)
NRM $\left(\times 10^{-5} \frac{emu}{g}\right)$	6.1
IRM_s^0 $\left(\times 10^{-3} \frac{emu}{g}\right)$	4.75
IRM_s^0/NRM	78
$TRM^1(H_{lab}) \times 10^{-5} \frac{emu}{g}$ (Oe)	3.36 (.087)
TRM^1/NRM	.55
H_0^1 (Oe)	0.16
IRM_s^1 $\left(\times 10^{-3} \frac{emu}{g}\right)$	48.1
IRM_s^1/IRM_s^0	10.1
$TRM^2(H_{lab}) \times 10^{-5} \frac{emu}{g}$ (Oe)	253 (.63)
TRM^2/NRM	41.5
H_0^2 (Oe)	.015
IRM_s^2 $\left(\times 10^{-3} \frac{emu}{g}\right)$	128
IRM_s^2/IRM_s^0	27

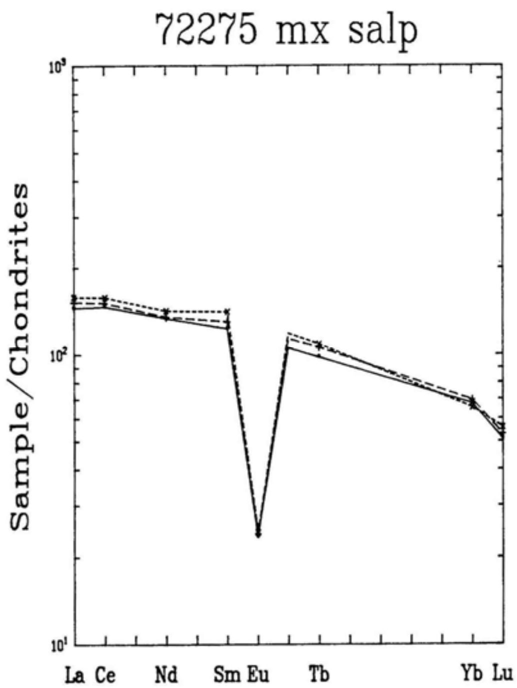

Figure 19b: Abundances of rare earth elements in 72255 friable matrix. These samples are all rich in KREEPy basalts, and may be pure KREEPy basalt breccias. Data from Table 5b (Salpas et al., 1987b).

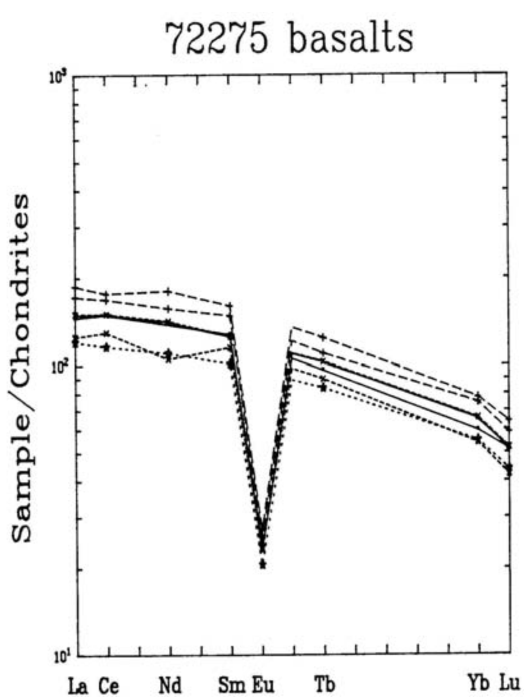

Figure 20: Rare earth elements in samples of KREEPy basalts and KREEPy basalt breccias. 72275,91 is the solid line near the middle of the range (Blanchard et al., 1975). The other five analyses are the two most REE-rich (#357 and 363b), the two most REE-poor (#393 and 359), and one close to an average composition (#347) from Salpas et al. (1987b).

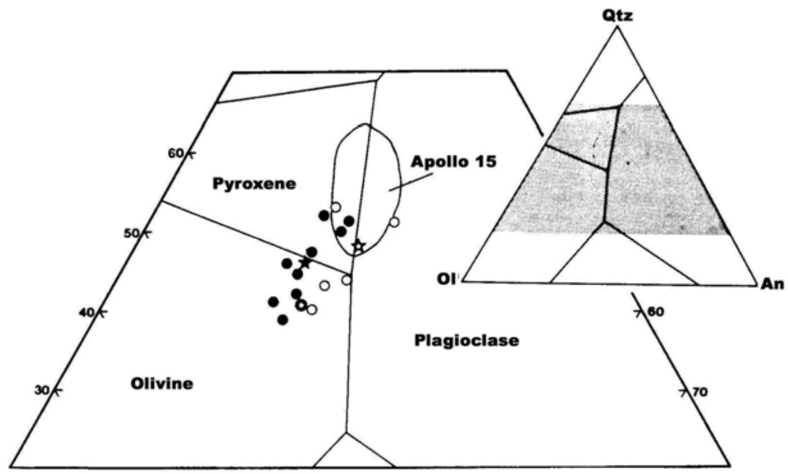

Figure 21: Pseudoquaternary phase diagram (0I-Si-An) far A 17 KREEPy basalts (Salpas et al., 1987b). The black dots are the 9 analyses that included major elements, with Si02 by difference; the filled star is the average of these 9 analyses. The enclosed star is the analysis of Blanchard et al. (1975). The open circles are defocused beam microprobe analyses of Ryder et al. (1977), with their average as an open star.

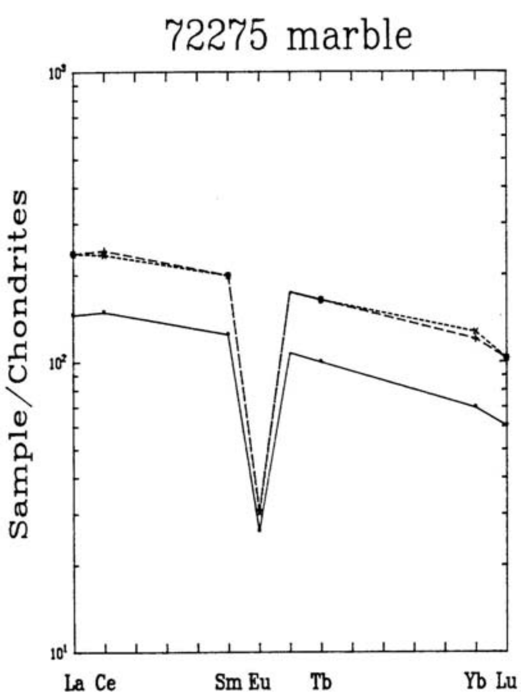

Figure 22: Rare earth elements in lithologies of clast #1 (Marble Cake clast). The two upper plots are for rind materials and are very similar. The lower plot is for the white interior, and probably includes a component of dark rind material. All data from Blanchard et al. (1975).

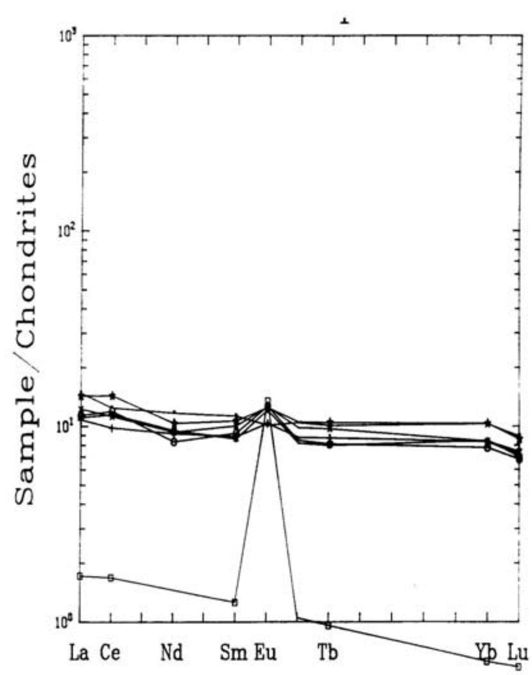

Figure 23: Rare earth elements in six felspathic granulites (top patterns) and a ferroan anorthosite (lower pattern) from 72275. Grid is drawn to conform as closely as possible with other diagrams in this section, so lower pattern falls below grid. Data from Salpas et al. (1987a).

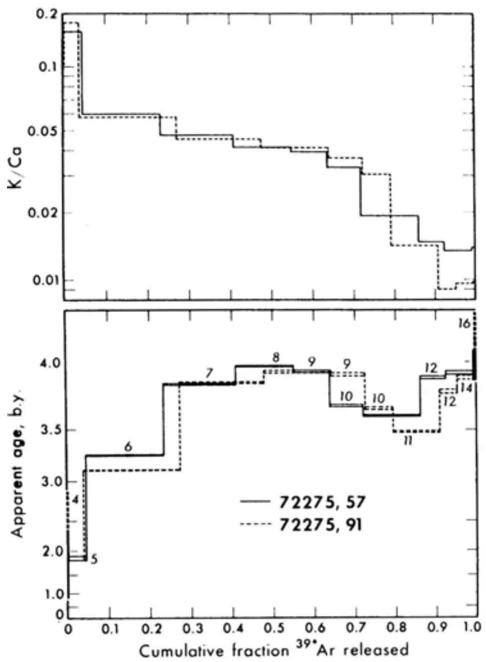

Figure 24: ^{40}Ar release diagram for 72275,57 (friable matrix) and 72275,91 (clast #5, KREEPy basalt). The apparent age scale is calibrated to the old decay constants. Leich et al. (1975a).

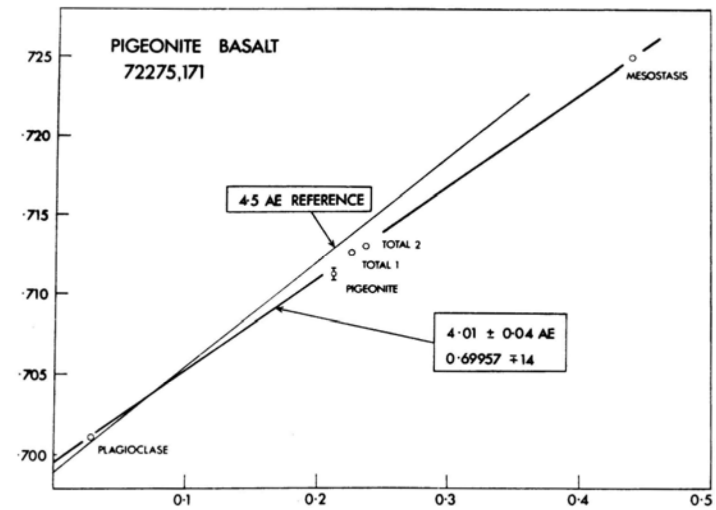

Figure 25a: Rb-Sr internal isochron for 72275 KREEPy basalt (probably clast #4). The age is 3.93 +/- 0.04 Ga with the new decay constants. Left hand axis is ^{87}Sr/^{86}Sr; lower axis is ^{87}R0^{6}Sr. Compston et al. (1975).

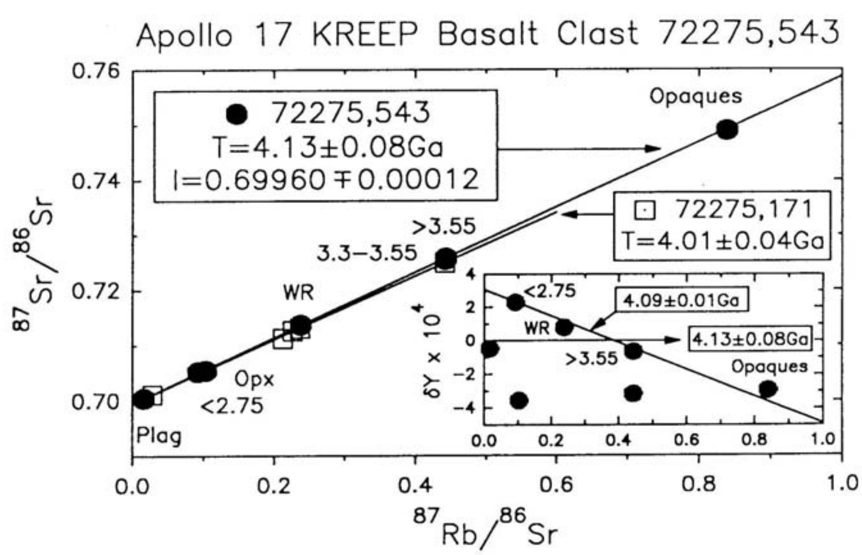

Figure 25b: Rb-Sr isochron for KREEPY basalt sample 72275,543. Ages calculated with old Rb decay constant. Shih et al. (1992).

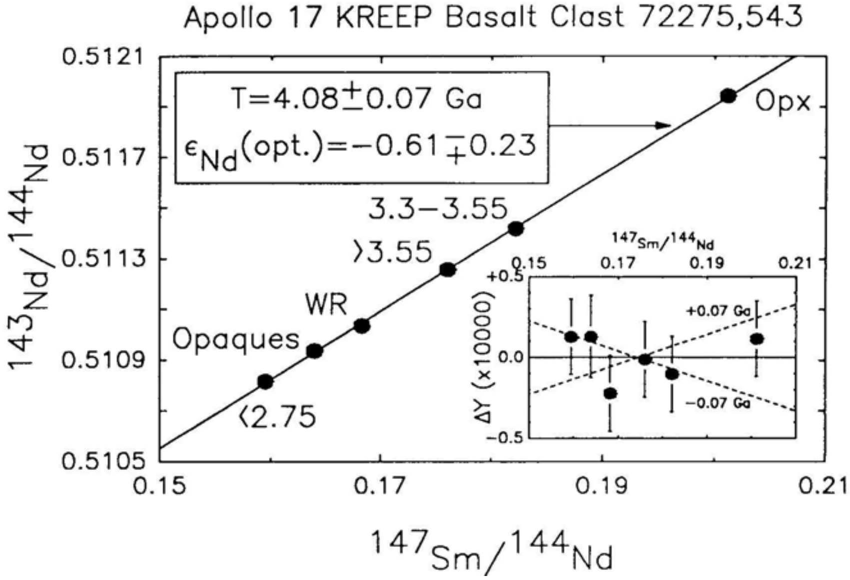

Figure 25c: Sm-Nd isochron for KREEPy basalt sample 72275,543. Shih et al. (1992).

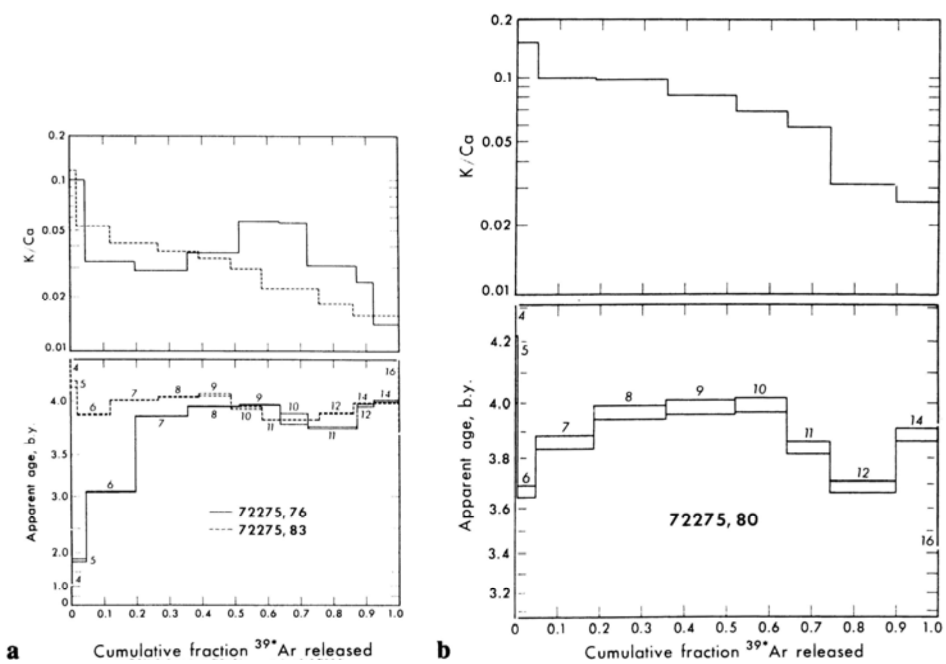

Fig. 26: Apparent ^{40}Ar age and K/Ca for 72275 samples. Age calibrations are with old decay constants. Leich et al. (1975b). a) 72275,76 (Marble Cake interior) and 72275,83 (dark melt breccia clast #2), b) 72275,80 (Marble Cake rind).

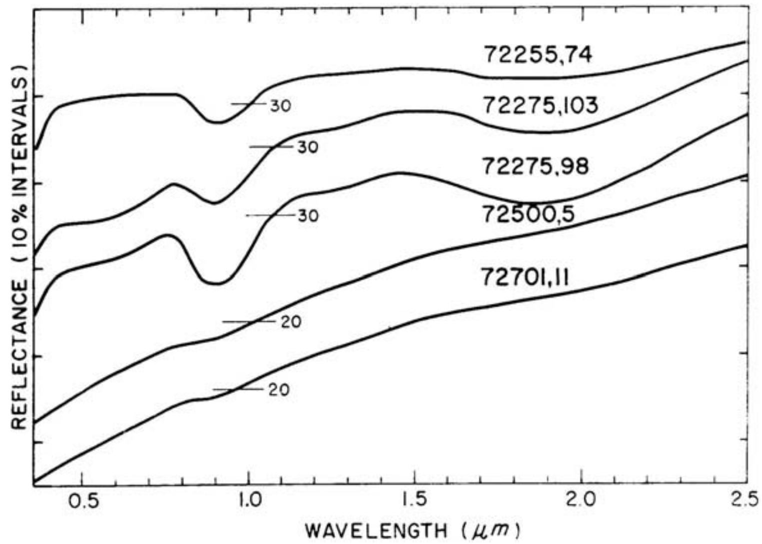

Figure 27: Diffuse reflectance spectra for 72275 and some other A 17 samples. Adams and Charette (1975).

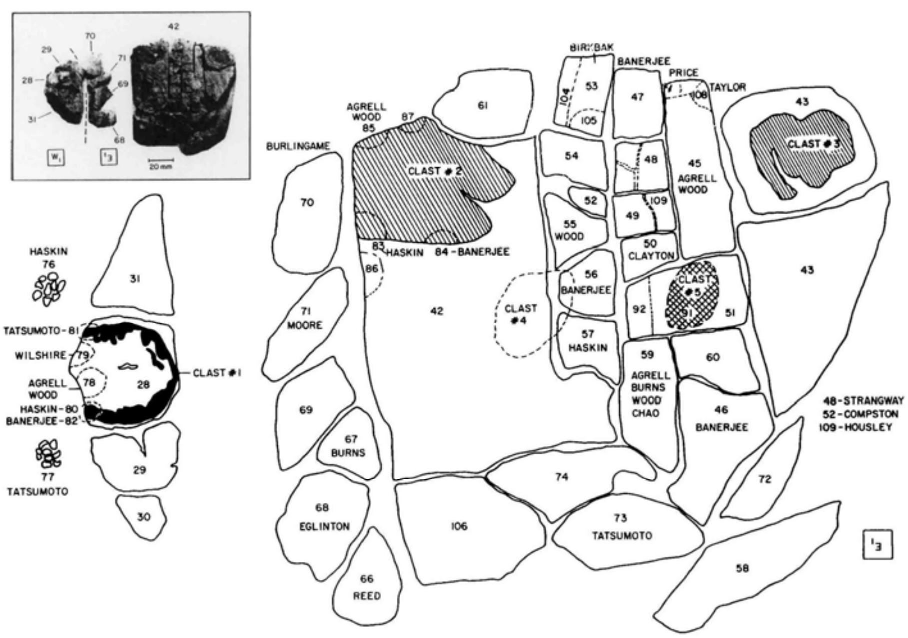

Figure 28: Subdivisions of 1973 slab 72275,42. (Marvin, in CI 2, 1974).